Nanomedicine: Nanotechnology, Biology, and Medicine
28 (2020) 102222

nanomedicine
Nanotechnology, Biology, and Medicine

nanomedjournal.com

The state of the art of nanopsychiatry for schizophrenia diagnostics and treatment

Allan Radaic, PhD[a,*], Daniel Matins-de-Souza, PhD[a,b,c,d]

[a]*Laboratory of Neuroproteomics, Department of Biochemistry and Tissue Biology, Institute of Biology, University of Campinas (UNICAMP), Campinas, Brazil*

[b]*Instituto Nacional de Biomarcadores em Neuropsiquiatria (INBION) Conselho Nacional de Desenvolvimento Científico e Tecnológico, Sao Paulo, Brazil*

[c]*Experimental Medicine Research Cluster (EMRC), University of Campinas, Campinas, SP, Brazil*

[d]*D'Or Institute for Research and Education (IDOR), São Paulo, Brazil*

Revised 18 March 2020

Abstract

Schizophrenia is one of the top 25 causes of global diseases burdens in terms of years lived with the disease and the emotional and economical strains it imposes on the society. Several strategies have been used to treat the patients, specially using typical and atypical psychoactives. However, due to its multifactorial characteristic and patient resistance, schizophrenia is still a difficult disease to diagnose and treat. Thus, new strategies for diagnostics and treatment must be researched to optimize the efficacy and reduce the side effects of the actual therapy. Nanomedicine tries to improve low-weight molecular agents for treatment of diseases through the use of nanoscaled carriers. Among nanomedicine, nanopsychiatry specifically deals with the potential role of nanotechnology in solving psychiatry diseases problems. Therefore, the objective of this work is to provide an overview of the state of the art of nanopsychiatry in the sense of treating schizophrenia.

Key words: Schizophrenia; Schizophrenia diagnostics; Schizophrenia treatment; Psychiatry; Nanomedicine; Nanopsychiatry; Nanotechnology

Psychiatry

Psychiatry is the medical specialty devoted to diagnosing, treating and preventing mental disorders. Mental illnesses comprise a broad range of medical conditions that affect the thoughts, emotions, behavior and relationship with the others. Mental diseases are often ignored or forgotten due to their small impact on mortality (0.5% proportion to total years of life lost compared to other illness, such as cardiovascular (15.9%), neonatal (11.2%) and cancer (10.7%) diseases).[1] However, it is estimated that 8 million deaths per year can be attributed to all mental illnesses globally for 2015,[2,3] a similar estimation for the total cancer deaths in the same year (8.7 million).[4] Besides this, it is estimated that 45% of the total population will eventually experience some psychiatric disorder during their lives.[1]

Among all the mental illnesses, schizophrenia is one of the top 25 causes of global diseases burdens in terms of years lived with the disease and the emotional and economical strain it imposes on society.[5] A recent study demonstrated that the annual cost of schizophrenia in the world ranged from US$94 million to US$104 billion.[6] Most of this expense came from indirect costs, such as absenteeism or sick leave (forgone work productivity), presenteeism (decreased work productivity), unemployment, permanent disability, and early retirement for patients, family members, or caregivers.[7] These indirect costs are especially relevant to schizophrenia patients, as schizophrenia is considered to have the highest disability weight among all other mental illnesses[1] and patient care is needed for the rest of the patient's life.[8]

Schizophrenia

Schizophrenia is a chronic disease that impacts significantly on cognition, social functioning and ability to work and is characterized by three main classes of symptoms: positive (i.e. delusions or hallucinations), negative (i.e. avolition and social withdrawal), and cognitive (i.e. impairment in working

This research was supported by the São Paulo Research Foundation (FAPESP) (grants #2013/08711-3, #2017/25588-1 and #2018/03673-0), and the Brazilian Coordination for the Improvement of Higher Education Personnel (CAPES) (grant #88887.200957/2018-00).

Conflict of interest: No potential conflict of interest was reported by the authors.

*Corresponding author at: Department of Biochemistry and Tissue Biology, Institute of Biology, University of Campinas (UNICAMP), Rua Monteiro Lobato, 255, Campinas, São Paulo, Brazil, 13083-862.

E-mail address: allan.radaic@gmail.com. (A. Radaic).

https://doi.org/10.1016/j.nano.2020.102222
1549-9634/

memory). It is considered a multifactorial disease, as there are genetic, developmental and environmental factors that could lead to the disease. However, due to poor medication efficacy and the fact that 20%-30% of the patients are estimated to be treatment resistant,[9,10] only 40% of the schizophrenic patients effectively respond to the traditional treatment.[11]

Besides these patient-related issues, development of new drugs for schizophrenia has limitations as current schizophrenia drugs present food interaction effects, limiting their period of usage[12] and, as approximately 70% of all newly discovered drugs present poor aqueous solubility, additional difficulty is inherited to develop new drugs for treating schizophrenia effectively.[1]

Therefore, new strategies to treat schizophrenic patients are being developed to optimize the current treatments and reduce their side effects. Among these new strategies, nanotechnology is having increased interest in the literature in recent years.

Nanotechnology and nanopsychiatry

Nanotechnology produces materials in the nanometric size range (1-1000 nm) that may present unique features compared with their bulk counterparts.[13–16] Due to the nanoscale physical proprieties, nanomaterials can present increased reactivity, reduction of thermal resistivity and the possibility of intracellular delivery of therapeutics. Therefore, these materials are being widely investigated for medical application.[17] These unique features have been so compelling that it led to the creation of the nanomedicine research field.[15,16]

Specifically, nanomedicine aims to improve the use of low-weight molecular agents, such as drugs, lipids, proteins and/or genetic materials as nanopharmaceuticals systems.[16,18] Among the nanomedicine research field, nanopsychiatry was first proposed by Fond and collaborators in 2013[19] for the potential role of nanotechnology in solving psychiatry diseases problems and is gaining increase interest in the literature. However, this specific term (nanopsychiatry) has only been used by 3 articles.[19–21]

Despite the specific term not being largely used in literature after 6 years of Fond et al publication, searching the MEDLINE database of references using PubMed research engine using the terms "nanotechnology" AND "detection" AND "psychiatry" together indicates a growing number of publications using both keywords from 2009 to 2017 (Figure 1). This indicates that nanopsychiatry has been gaining increasing interest in recent years (3.5-fold increase of the normalized number of articles between 2017 and 2014 and a 10-fold increase between 2017 and 2013), thus demonstrating the potential for the nanotechnological growth for future treatment of mental illnesses.

Therefore, the objective of this work is to provide an overview of the state of the art of the nanotechnological or nanopsychiatric approach to treat schizophrenia.

Nanopsychiatry for schizophrenia diagnostics

Since schizophrenia diagnostics is rather intricate and it is challenging to diagnose due to the disease complexity, nanopsychiatry research field might assist the diagnosis of the disease. Our literature research demonstrated that the majority

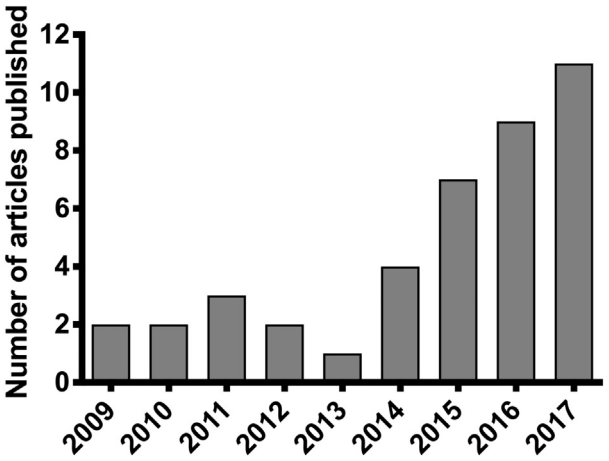

Figure 1. Increase of the published articles on MEDLINE database using the PubMed search engine using the terms "Nanotechnology" AND "detection" AND "psychiatry" normalized by 100,000 published articles on the database per year between 2009 and 2017. Research done on October 1, 2019.

(>90%) of research articles for schizophrenia diagnosis focused on creating reliable dopamine and serotonin detection methods with lower detection limits than traditional methods. Next, we will discuss the nanopsychiatry for dopamine detection.

Dopamine detection

Dopamine is considered one of the most important neurotransmitters because it has valuable roles in functioning of the central nervous, hormonal and renal systems. Thus, disturbances in dopamine level are directly correlated to neurological disorders, such as schizophrenia, Parkinson's, Alzheimer's and Huntington's diseases, Tourette syndrome and epilepsy.[22–25] Specifically, for schizophrenia, it was hypothesized in the 1960's that dopamine overactivity might be the common denominator of the psychotic episodes in schizophrenia (hyperdopaminergic state).[26] This is known as the dopamine hypothesis and is one of the most enduring hypotheses in psychiatry.[26,27] Interestingly, dopamine regulation is used as schizophrenia treatment by the blockade of the dopamine receptors 1 and 2 in the brain by antipsychotics. Therefore, dopamine level determination might be vital for diagnosing and treating schizophrenia.[23–25]

Interestingly, the majority of the research articles found (~74%) during the writing of this work are related to the nanotechnological approach to detect dopamine, which might be related to this huge implication of dopamine in schizophrenia.

Extraordinarily, there is a plethora of methods to detect dopamine, such as electrophoresis, high performance liquid chromatography (HPLC) and chemiluminescence.[25,28,29] However, these methods have several limitations, such as expensive instrumentation, low portability, and complex and time-consuming sample pre-treatment.[24,25] Therefore, new strategies for dopamine detection are needed in order to mitigate those limitations.[25] A summary of the nanotechnological approaches for dopamine detection found in literature can be seen on Table 1.

Interestingly UV-vis was the most used technique to determine the dopamine levels (represented in 33% of all of

Table 1
Nano-sized approach to dopamine detectors found in literature.

Author	Nanoparticle characteristics		Detection characteristics			
	Type of nanoparticle used	Mean nanoparticle diameter (nm)	Detector type	Detection linear range (nM)	Limit of detection (nM)	Sensibility increase[a]
Wang et al, 2013[30]	Magnetic iron oxide and gold nanoparticles	12.8	UV-vis spectra	20-800	10	NR
Biswal et al, 2013[31]	Polymethacrylate-capped silver nanoparticles	6	UV-vis spectra	158-52,700	158	NR
Qian et al, 2013[32]	Gold nanoparticles-coated polystyrene/reduced graphite oxide microspheres	Gold nanoparticles: 5; whole nanoparticle: 200-220	Electrochemical	50-20,000	5	NR
Amiri et al, 2014[33]	Cysteine-functionalized carbon nanoparticles	20-40	Electrochemical	10-10,000	3.6	NR
Qian et al, 2014[34]	Gold nanoparticles-coated polypyrrole/reduced graphite oxide sheets	80	Electrochemical	0.1-5000	0.01829	NR
Leng et al, 2015[35]	Gold nanoparticles + thioglycolic acid	<50	UV-vis spectra	100-1000	Naked eye: 100 nM in MilliQ water; UV-vis: 33 nM (in Milli-Q water), 100 nM (in urine) and 94 nM (in serum)	5.6-fold (in urine); 10-fold (in blood)
Liu et al, 2015[36]	Palladium-loaded iron oxide III nanoparticles	50	Electrochemical	NR	20,000	NR
Zhang et al, 2015[29]	(3-Aminopropyl) trimethoxysilane–silicon nanoparticles	2.4	Fluorescence	5-10,000	0.3	NR
Zhang et al, 2016[37]	Gold nanoparticles + 6-carboxyfluorescein-labeled aptamers	~13	Aptamers	Colorimetric: 170-4000 Fluorescence: 83-2000	Colorimetric: 140 Fluorescence: 78.7	NR
Khudaish et al, 2016[38]	Poly(2,4,6-triaminopyrmidine) film decorated with gold nanoparticles	30	Nanoelectrode	150-1500	17	NR
Liu et al, 2017[39]	Gold nanoparticle-sheathed glass capillary	15-160	Nanoelectrode	NR	49	NR
Iswarya et al, 2017[23]	L-histidine-capped gold (AuNP), silver (AgNP) and gold–silver ((Au–Ag)NP) nanoparticles	AuNP: 11; AgNP: 5; (Au–Ag)NP: 6.5	UV-vis spectra	100-2500	NR	NR
Alexander & Bandyopadyay, 2017[40]	Palladium nanoparticles	7.8	Electrochemical	50-130,000	25	NR
Li et al, 2018[25]	Oligonucleotides-conjugated gold nanoparticles	Unconjugated: 12; conjugated: 25	Microcantilever	500-4000	77	15-fold
Mei et al, 2018[41]	Gold nanoparticles	10-150	Nanoelectrode	100-10,000	64.3	NR
Rostami et al, 2018[42]	Functionalized silver nanoparticles	40	UV-vis spectra	100-7500	31	NR
Lin et al, 2018[43]	L-cys-functionalized zinc nanoparticles	4.5	UV-vis spectra	26,300-68,500	791	NR
Qu et al, 2018[44]	Dual emission carbon dots and gold nanoparticles	Carbon dots: 2.08; gold nanoparticles: 18.01	Fluorescence	Blue emission: 500-3000; yellow emission: 100-3000	Blue emission: 230; yellow emission: 37	NR

NR = not reported by the authors.
[a] Compared to non-nanoparticulated systems (if any), as described by the author.

the articles found). Conversely, electrochemistry and fluorescence presented the lowest detection limits for dopamine, with 18.29 and 300 pM, respectively.

Figure 2 shows the relative abundance of nanoparticle types used by the articles cited in Table 1. We found that the majority (>50%) of the articles use gold nanoparticles, while less than

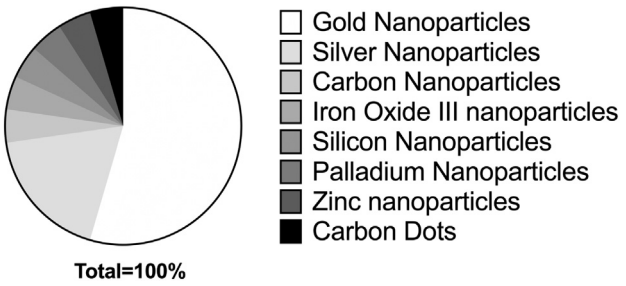

Figure 2. Relative share of the type of nanoparticles among the researched articles related to dopamine detection cited in this work.

10% of those use organic nanoparticles. Substances at the nanometric range do have different properties compared to their bulk counterparts, such as increased reactivity and surface area and reduction of thermal resistivity.[16] Particularly for dopamine and serotonin quantification, metallic nanoparticles seem to be better suited for this task than organic nanoparticles, as they present good electrochemical performance towards dopamine detection, including high sensitivity, good selectivity and low limit of detection[23,45,46]; thus, the higher use of metal nanoparticles over organic nanoparticles might be related to these facts. However, little is still known about how these nano-detectors increase the sensitivity of dopamine and serotonin detection.

Interestingly, these higher sensing capabilities of metal nanoparticles can be demonstrated by the fact that gold nanoparticles decorated polypyrrole/reduced graphene oxide hybrid sheets presented the lowest linear range (0.1-5000 nM) and minimum dopamine detection levels (18.29 pM).[34]

Li et al[25] built a microcantilever, a nanotechnological transducer that emits electronic signals when analytes interact with the microcantilever surface. To interact with aptamers, single-stranded oligonucleotides are capable to bind to the surface of the microcantilever. However, as dopamine has low molecular weight and a simple chemical structure, detecting dopamine only with the aptamer–microcantilever setup has difficulties to precisely determine the amount of the neurotransmitter. To solve this issue, the authors used oligonucleotides-conjugated gold nanoparticles as a signal amplifying strategy. In this strategy, the oligonucleotide present on AuNP was a complementary sequence of the aptamers. So, initially, the oligonucleotide-conjugated AuNP presented as combined to the aptamer on the surface of the microcantilever. In the presence of dopamine, the aptamers release the AuNP and bind to dopamine. The non-conjugated AuNP presented about 12 nm while the oligonucleotide-conjugated AuNP presented about 25 nm, indicating the conjugation between the oligonucleotides and the nanoparticles. By using this strategy, the authors increased the sensibility of the microcantilever by 15-fold compared to the system without nanoparticles.

Iswarya et al[23] developed dopamine detection method using L-histidine-capped gold (AuNP), silver (AgNP) and gold–silver ((Au–Ag)NP) nanoparticles. These metallic nanoparticles interact with dopamine, which can be detected by a shift of the surface plasmon resonance (SPR) of the nanoparticles. The average diameter found for L-His capped AgNP, AuNP, (Ag–Au)NP nanoparticles was 11 nm, 5 nm, and 6.5 nm, respectively. After characterizing the nanoparticles, the authors proceeded to dopamine detection. Analyzing the UV-vis spectra, the authors found a direct correlation between the wavelength and absorbance with dopamine concentration, which can be used for dopamine detection in the 10-25 μM range.

Leng et al[35] obtained a colorimetric array based on gold nanoparticles for dopamine detection on serum and urine. Interestingly, the dopamine detection can be made either by naked eye, with a limit of detection of 100 nM in MilliQ water, and/or by UV-vis spectrophotometry, with lower limit of detection in Milli-Q water (33 nM) and other body fluids, such as urine and serum, with a limit of detection of 100 nM and 94 nM, respectively. The probes were also found to be dopamine selective for detection among 22 biomolecules and ions at the 1000 nM concentration.

Serotonin detection

Although the dopamine hypothesis explains the main positive symptoms of schizophrenia, specially the psychotic episodes, it does not clarify the negative and cognitive symptoms of the disorder.[47,48] Thus, the serotonin hypothesis was created based on the efficacy of the atypical antipsychotic drugs, which act via dopaminergic and serotoninergic pathways.[47] According to this hypothesis, one of the upstream causes of schizophrenia is a stress-induced serotonin overdrive in the brain, disrupting the cortical neuronal function.[48] As the atypical antipsychotic drug acts on the serotoninergic pathway, serotonin detection may be a good prognostic tool for schizophrenia treatment. A summary of the nano-sized approach for serotonin detection found in literature can be seen on Table 2.

Figure 3 shows the relative share of the nanoparticle types cited in Table 2 for serotonin detection. We found that half (50%) of the journal articles in this field uses gold nanoparticles and none of them uses organic nanoparticles. This may be related to the fact that metal nanoparticles have better electrical–chemical sensing properties than organic nanoparticles.[23,45,46] This is interesting because >60% of the serotonin sensing technologies presented here are by electro-chemical reaction to the amount of serotonin in solution. Other serotonin sensing technologies, such as fluorescence, UV-vis and aptamer, are still used, however, with lower share of the publication (~12.5% each).

Interestingly, both of the most powerful detectors developed were using electrochemical sensors. Anithaa et al[54] presented a broader detection liner range (10 to 600,000 nM of serotonin) with a lower detection limit (1.42 nM of serotonin). This was done by coating the glassy carbon electrodes surface with gamma ray-irradiated tungsten trioxide nanoparticles as nano-sensor. The gamma ray-irradiated tungsten trioxide nanoparticles act as serotonin oxidizer, by transferring electrons to the serotonin molecules and releasing water in the process. Then, a cycle voltammetry can be used to detect the reactions in the phosphate saline buffer, which is limited by the amount of serotonin in the sample. To demonstrate the clinical application of this sensor, the authors added known amounts of serotonin in

Table 2
Nano-sized approach for serotonin detectors found in literature.

Author	Nanoparticle characteristics		Detection characteristics			
	Type of nanoparticle used	Mean nanoparticle diameter (nm)	Detector type	Detection linear range (nM)	Limit of detection (nM)	Sensibility increase[a]
Xue et al, 2014[49]	Gold nanoparticles embedded on r educed graphene oxide/polyaniline nanocomposites	93	Electrochemical	200-10,000	11.7	NR
Cesarino et al, 2014[50]	Carbon nanotubes/polypyrrole/silver nanoparticles nanohybrid	750	Electrochemical	500-5000	150	2 to 5-fold
Chavez et al, 2017[51]	Gold nanoparticles	~15	Aptamer/ UV-vis spectra	750-2500	300	NR
Ran et al, 2017[52]	Iron oxide III nanoparticles	NR	Electrochemical	500-100,000	80	NR
Tertis et al, 2017[53]	Polypyrrole and gold nanoparticles	Polypyrrole nanoparticles: 100-200 Gold nanoparticles: 20-32 Unrradiated: 40	Electrochemical	100-15,000	33.22	320-fold
Anithaa et al, 2017[54]	γ-Irradiated tungsten trioxide nanoparticles	50 kGγ: 51 100 kGγ: 21 150 kGγ: 53	Electrochemical	10-600,000	1.42	NR
Swain et al, 2018[55]	Silver nanoparticles	8.7	Fluorescence	NR	50,000	NR
Godoy-Reyes et al, 2018[56]	Dithiobis(succinimidylpropionate) and N-acetyl-l-cysteine functionalized gold nanoparticles	15	UV-vis spectra	100-3000	100	NR

NR = not reported by the authors.
[a] Compared to non-nanoparticulated systems (if any), as described by the author.

blood serum samples. Remarkably, the sensor was able to detect the serotonin amounts with less than 3% error in the blood serum sample.

In a similar fashion, Tertis et al[53] developed a graphite based electrode associated with polypirrole polymeric nanoparticles decorated with gold nanoparticles. Although the authors do not discuss how these nano-sensors in fact detect the amount of serotonin in the sample, the sensor presented a higher linear range (100 to 15,000 nM) and detection limit (33.22 nM) than the tungsten trioxide nanosensor. Even so, Tertis et al demonstrated that the nano-sensor was 320-fold more sensitive than the bear graphite electrode in blood serum, thus underlining the potential of this nano-sensor and demonstrating how nanopsychiatry can assist the development of more sensitive serotonin sensors.

Interestingly, most of the dopamine and serotonin detectors cited here did not report any comparison between their developed system efficiency to a non-nanoparticulated sensor. However, the ones that compared their systems indicated an impressive sensitivity improvement (up to 350-fold increase). Thus, more studies are still needed to compare and demonstrate that these new sensors can indeed increase dopamine and serotonin sensitivity.

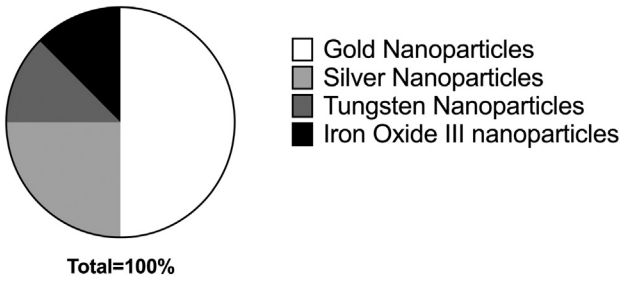

Figure 3. Relative share of the type of nanoparticles used in the researched articles related to serotonin detection cited in this work.

Detection of epigenetic modifications in genomic DNA

It has been demonstrated that genetic and environmental factors, like epigenetic factors, seem to play a role in schizophrenia.[57] Among the epigenetics factors, DNA methylation is one of the well-characterized and stable epigenetic modifications.[58]

The work by Shimabukuro et al[59] was the starting point of DNA methylation markers' discovery in schizophrenic patients. The authors indicated that peripheral blood of male schizophrenic patients was hypomethylated. Today, the main candidates for DNA methylation profiles related to schizophrenia are concentrated on genes associated with specific neurotransmitter-related systems, such as gamma-aminobutyric acid (GABA), glutamate, serotonin, and dopamine systems. Besides that, there are methylome-wide association studies for schizophrenia methylation targets. To read more on the progress and perspectives of DNA methylation analysis in schizophrenia, read Zong et al[58] and for a complete list of possible gene candidate as well as for the methylome-wide target studies for schizophrenia, read Pries et al.[57]

Regarding the nano-sized approach for DNA-methylation detection, it has been demonstrated that methylation-specific quantum dots associated with fluorescence resonance energy transfer (FRET) can detect the methylation status of a DNA molecule (Figure 4).[60,61] Briefly, sodium bisulfite is used to convert unmethylated cytosines into uracil while methylated

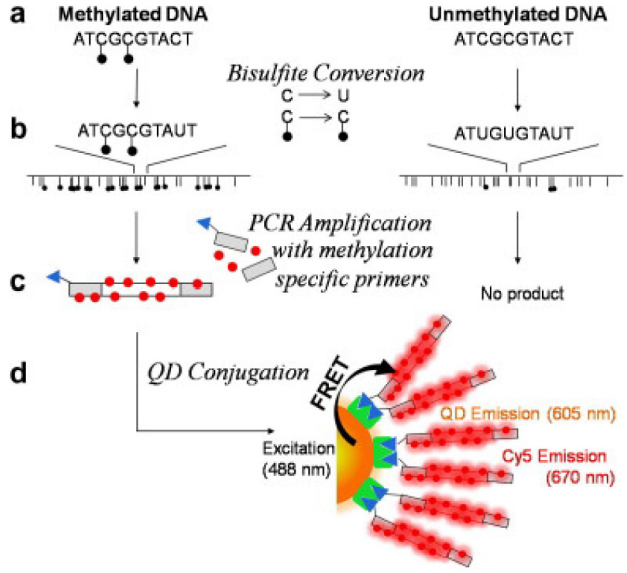

Figure 4. Schematic depiction of methylation detection via MS-qFRET. **(A)** Representative methylated and unmethylated genomic DNA sequences. **(B)** Sodium bisulfite conversion of unmethylated cytosines into uracil while methylated cytosines remain unconverted. **(C)** PCR amplification is methylation dependent as a result of primer sequencing and the variation between bisulfite treated DNA. Cy5-dCTP (red dot) incorporates throughout the target sequence of each amplicon. Forward primers contain a biotin label (blue triangles) for post-PCR conjugation to quantum dots. Unmethylated DNA template does not get amplified with methylation-specific primers. **(D)** Target is conjugated to quantum dot (FRET donor) by biotin–streptavidin affinity. Upon excitation at 488 nm, QD emission is recorded at 605 nm and Cy5 (FRET acceptor) at 670 nm. Reproduced from Bailey et al[61] under the License Number 4695060569769.**Reprinted from Vasudev J. Bailey, Brian P. Keeley, Christopher R. Razavi, Elizabeth Griffiths, Hetty E. Carraway, Tza-Huei Wang, *DNA methylation detection using MS-qFRET, a quantum dot-based nanoassay*, pp.237-241 Copyright 2010, with permission from Elsevier.

cytosines remain unconverted in the DNA sample. Using methylation-dependent PCR amplification primers, Cy5-dCTP is incorporated throughout the DNA sample together with a forward primer containing biotin. The biotin is then used to couple with the quantum dots via biotin–streptavidin affinity, thus promoting FRET on the methylated locations. On the other hand, unmethylated DNA is not amplified, resulting in no conjugation and, thus, no FRET is displayed. This technique, called methylation specific quantum dot fluorescence resonance energy transfer (MS-qFRET), improves the sensitivity of the methylation detection and quantification due to its low background noise and high signal promoted by the quantum dots FRET.

Using a different approach, Wang et al[62] demonstrated that a tetramethylammonium-based nanopore (TMA-NP) sensor can accurately detect locus-specific DNA methylation without bisulfite conversion, chemical modification or enzyme amplification (Figure 5). Briefly, TMA+ is a quaternary ammonium cation, comprising four methyl groups attached to a central nitrogen atom and is used as a supporting electrolyte in organic electrochemistry. The authors produced a TMA nanopore with a specific diameter (1.4 nm), which is smaller than a double stranded DNA (2.2 nm), but larger than a single stranded DNA (1.2 nm). As the hairpin DNA is driven into the pore, the duplex part of the hairpin is trapped outside of the nanopore. As electric field force is applied, the hairpin unzips and translocates through the nanopore. Interestingly, methylated hairpin unzipping and translocation through the nanopore were faster than the unmethylated hairpin. For instance, one distinct methylation point in the DNA hairpin decreases the translocation time through the nanopore by 3-fold and two distinct methylations in the DNA hairpin decrease the translocation time by 17-fold. The hairpin dwell time can be measured and used to quantify the amount of methylation in the DNA. To analyze a coding gene (i.e. tumor suppressor gene P16 (CDKN2A)), the authors needed to fragment the gene into 13-nucletiode fragments and then analyzed the amount of methylation each fragment had. However, this fragmentation step could promote difficulties on the analysis of a locus in genomic DNA for schizophrenia to exactly know which fragment is passing through the nanopore at that exact moment and, thus, know which fragment of the locus is methylated or not.

Antibodies

Although antibodies can be used to diagnose, predict or prognose psychotic disorders, to date, there is no specific biomarker for schizophrenia due to the complexity of the disease.[63] Proteomics and pluripotent stem cell technology have been aimed to unveil and validate biomarkers for the schizophrenia.[11] Once these biomarkers are well established, nanoparticles are able to be decorated/conjugated with antibodies in order to help/improve detection, targeted delivery and antibody half-life. For instance, epidermal growth factor receptor (EGFR) antibodies attached to gold nanoparticle were used as a computed tomography contrast agent to distinguish benign from malignant lung cancer nodules.[64] The rationale is that the malignant lung cancer present overexpressed EGF receptors, which could be used to distinguish between benign and malign nodules. As result, the antibody-attached nanoparticle had significant tumor accumulation compared to no-antibody nanoparticle. Using a similar strategy, one can use an antibody-decorated nanoparticle to bind to a schizophrenia biomarker and, thus, effectively determinate which patients present schizophrenia or not, or even screen potential-to-be schizophrenic patients.

Nanomedicine for schizophrenia treatment

Antipsychotic are a class of drugs usually used to treat the positive and negative symptoms of schizophrenia. Some of these drugs can be used to treat other diseases, such as chlorpromazine, which can be used to treat the maniac phase of the bipolar disorder as well.

The first type of antipsychotic discovered (also called typical antipsychotic) acts on the dopaminergic system, blocking the dopamine type 2 (D2) receptors in the brain.[65] The main typical antipsychotic drugs are chlorpromazine and haloperidol. However, typical antipsychotics usually induce side effects, namely, extrapyramidal side effects (EPSE). Among these EPSE, drug-

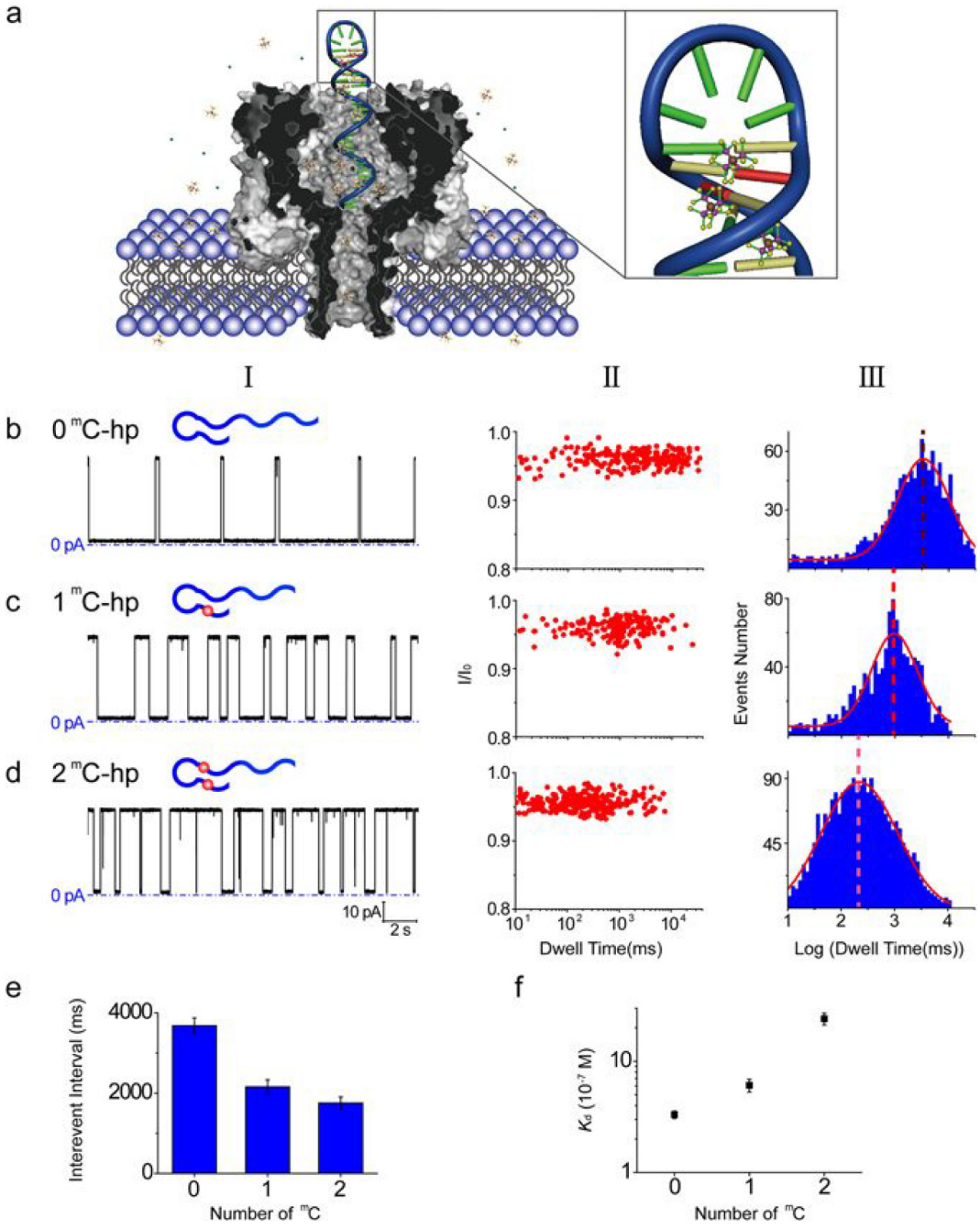

Figure 5. TMA-NP discrimination of unmethylated and methylated DNA. **(A)** Schematic of the methylated DNA hairpin containing two 5′-methylcytosines (red) at duplex (2 mC-hp) translocating through the wild-type α-hemolysin (α-HL) nanopore in 4 M TMA-Cl. **(B-D)** Representative single-channel recording traces (column I), scatter plot of I/I0 vs dwell time (column II) and dwell time histogram in log form (column III) for unmethylated DNA (0 mC-hp) **(B)**, methylated DNA containing one 5′-methylcytosine (1 mC-hp) **(C)** and two 5′-methylcytosines (2 mC-hp) **(D)** in 4 M TMA-Cl. 5′-Methylcytosine is shown as red circles. The signals were filtered at 2 kHz and sampled at 20 kHz. Scatter plot and dwell time histograms are collected from 300 events. I/I0 is normalized blockage current, which was obtained by dividing the average blockage current of an event by the average open channel current. The distribution of the dwell time histogram was fitted to a Gaussian function. Reproduced from Wang et al.[62]

induced movement disorders such as parkinsonism, dystonia and tremors are the most prominent.[65] Later on, it was discovered that antipsychotic EPSE and D2 receptor antagonism were linked together for these drugs.[66]

More recently, the second-generation antipsychotic (also called atypical antipsychotics) has become available. Atypical antipsychotics have lower affinity and occupancy to the dopaminergic receptors and higher occupancy to the serotoninergic receptors, compared to typical antipsychotic.[65] Interestingly, this lower dopaminergic blockade of the atypical antipsychotics induces less extrapyramidal side effects, compared to the typical antipsychotic.[65]

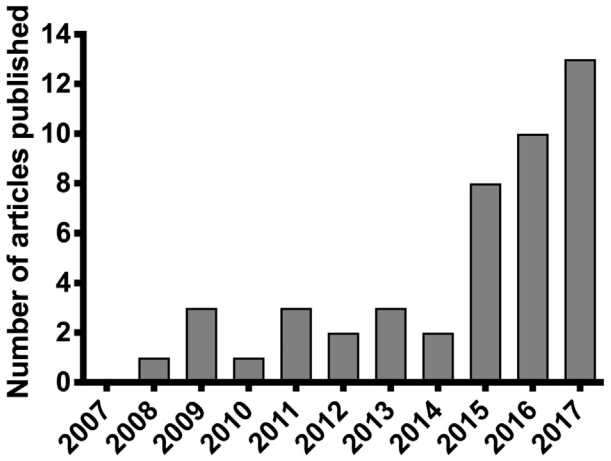

Figure 6. Increase of the published articles on MEDLINE database using the PubMed search engine using the terms "Nanotechnology" AND "treatment" AND "psychiatry" normalized by 100,000 published articles on the database per year between 2009 and 2017. Research done on October 1, 2019.

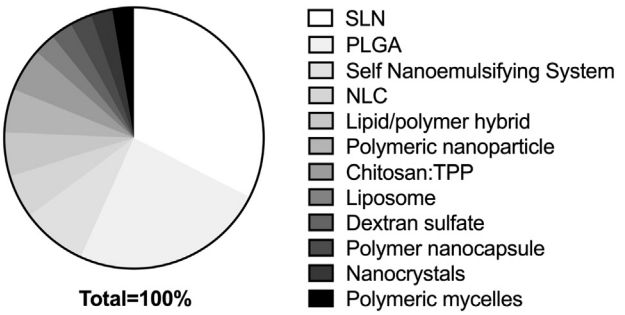

Figure 7. Relative share of the type of nanoparticles used in the researched articles related to schizophrenia treatment cited in this work.

Nanopsychiatry, through the use of nanoscale drug delivery systems (nano-DDSs), can increase the efficacy of antipsychotics by mitigating their specific drawbacks, such as low bioavailability, plasma half-life and water solubility.[1] These nano-DDSs are designed to modify the pharmacokinetics and biodistribution of their active load, protecting it from degradative enzymes and promoting a sustained release of the active by acting as drug reservoir inside the body.[67] Despite that, nanopsychiatry can assist schizophrenia treatments by decreasing the drug EPSE by increasing the tissue targeting efficiency and, thus, reducing the amount of drug needed to reach the target site.

Searching the MEDLINE database of references using PubMed research engine using the terms "nanotechnology" AND "treatment" AND "psychiatry" together indicates a growing number of publications using the both keywords from 2007 to 2017 (Figure 6). This indicates that nanopsychiatry has been gaining increasing interest in recent years, especially after 2015 (6-fold increase of the normalized number of articles between 2017 and 2014 and a 9.5-fold increase between 2017 and 2011). Interestingly, lower numbers of research articles research were found before 2009, which might correlate with the 2009 FDA approval of the first nanopsychiatry product, the Invega Sustenna® (Janssen Pharmaceuticals Inc., NJ, USA). The Invega Sustenna® is a paliperidone nanocrystal formulation administrated monthly via intramuscular injection.[68,69]

Thus, demonstrating the potential growth of nanotechnological devices to diagnose mental illnesses.

Among our research, we find out that olanzapine (an atypical antipsychotic) seems to be the most studied drug for nanopsychiatry (representing 18.4% of all traditional antipsychotic nano-DDSs) followed by quetiapine and clozapine (each representing 15.8% of all traditional antipsychotic deliveries) and then risperidone (representing 13.1% of all traditional antipsychotic deliveries). All of these drugs belong to the atypical antipsychotics and, except quetiapine, are the most effective agents to treat schizophrenia psychosis.[66] Interestingly, the most used nano-DDSs were solid lipid nanoparticles (SLN), with 32.43% of the articles cited, followed by poly(lactic-co-glycolic acid) (PLGA) nanoparticles, with 24.32%, as Figure 7 shows.

Compared to the free drug, all studies found here demonstrated increased AUC and Cmax, but not all of them reported increased Tmax.[70–75] This is rather intriguing, as one of the major advantages for nanoparticle formulation is the possibility of sustained or controlled drug release.[76] Interestingly, most of the *in vitro* drug release studies reported release of the majority of the drug load between the first 5 min and 24 h, with only 3 studies indicating sustained drug release.[77–79] It is possible that this formulation presented the majority of the drug load located on the surface of the nanoparticle, thus promptly releasing the majority of the drug in the first few hours.[76]

Comparing these studies to Invega Sustenna®, except for Miao et al,[75] the majority of these studies seem to not reach the same level of Tmax, Cmax or AUC found on the FDA approved formulation. For instance, Seju et al[80] and Vieira et al[70] found a Tmax of 60 min and 16 h. Seju et al, found a Cmax of 200 ng/mL after a 1.45 mg/kg intranasal injection, while Veira et al found an AUC of 8188 ng h/mL after a 5 mg/kg injection. According to the pharmacological and toxicological review and evaluation of the Invega Sustenna® formulation made by the Center of Drug Evaluation and Research/FDA and published in 2009,[81] the Invega Sustenna® has a Cmax of 662 ng/mL, Tmax of 192 h and AUC of 153,000 ng. h/mL in rats after 160 mg/kg injection. However, the comparison between the majority of the studies found here and Invega Sustenna® results might be complex as no other study, rather than Miao et al, tested a similar dose to Invega Sustenna formulation. Most of the studies found here tested doses between 0.3 mg/kg and 40 mg/kg; therefore, upscaling the dosage of these studies may be necessary to fully compare these formulations. Miao et al,[75] on the other hand, found Cmax of 1,902,000 ng/mL, Tmax of 1 h and AUC of 4,195,000 ng h/mL after a dose of 134 mg/kg. This represents a 2800-fold increase on Cmax and 27-fold increase on AUC compared to Invega Sustenna.

Table 3 summarizes all the findings regarding nano-DDS schizophrenia treatments. Next, we deeply discuss each of the major typical and atypical antipsychotics used in nanopsychiatry.

Typical antipsychotic delivery

Chlorpromazine

Chlorpromazine was the first antipsychotic discovered[66] and presents low bioavailability (30%-50%) due to its first pass metabolism in the liver.[77] To overcome this drawback, Halayqa et al[77] synthesized 9 different PLGA nano-DDSs for chlorpromazine delivery and the morphology of 3 of those nano-DDSs formulations is shown in Figure 8. The authors used different amounts of PLGA as well as the sonication power used to produce the different formulations. The encapsulation efficiency of these formulations ranged from 44.8% to 71.0% but the formulation containing the lowest amount of PLGA presented an initial burst release of ~90% of chlorpromazine within the first 6 h. Then, the remaining amount (~10% of the chlorpromazine load) was released by a diffusion until 48 h.

The formulations with higher amount of PLGA presented the same initial burst effect, but the majority of the drug (>70%) was released within 16 h. Although burst releases on PLGA polymeric nanoparticles are well documented in literature, no consensus has been achieved in the underlying mechanism of it.[107,108] De Azevedo et al[108] systematically studied the burst release effect in PLGA polymeric nanoparticles in more the 150 research articles in the literature. Interestingly, they found that the amount and the molecular weight of PLGA seem to be correlated to extending the release of the drug during burst releases.[108] This seems to be demonstrated here with PLGA nanoparticles for chlorpromazine release as increasing the amount of PLGA (from 0.8% to 1.6%) extended the drug release from 6 h to 16 h. Regarding the mechanism of the burst release, Halayqa et al argue that the pH of the aqueous solution containing the drug reduced the final poly-lactic polymer matrix of the final nanoparticle, degrading the majority of the nanoparticles. De Azevedo argues that encapsulation efficiency plays a significant role in bursts effect in PLGA nanoparticles, as the amount of initial burst release depends on the ability of the polymer matrix to solubilize the drug, thus making it unavailable for immediate diffusion. They also suggest that increasing the encapsulation efficiency of chlorpromazine would decrease the burst release as well. In the case of pH degrading the polymeric nanoparticles, using other kinds of nanoparticles, such as lipid nanoparticle, can prevent the burst release, as they are stable from pH 1 to 9.[109,110]

Haloperidol

Haloperidol is one of the most used typical antipsychotics.[97] However, due to high plasma-protein binding of the drug (~90%),[97] haloperidol penetration in the brain is reduced, as it has been demonstrated that the drug needs to be in its free state to cross the blood–brain barrier.[111] To overcome this drawback, maleimide-functionalized polymeric nanoparticles formed by PLGA decorated with poly-ethylene glycol (PEG-PLGA)[79] and solid lipid nanoparticles (SLN)[97] nano-DDSs have been developed for haloperidol delivery. Although similar encapsulation efficiency was obtained by both nano-DDSs (73% to 82.5% for PEG-PLGA and 68.4% to 71.6% for SLN), different drug release patterns were found. For PEG-PLGA, only 7.5% of drug load was *in vitro* released after 96 h, while SLN presented a faster *in vitro* release, with more than 80% of the drug load released at 24 h. The difference, however, can be due to different amounts of haloperidol added to both nano-DDSs, as 14-fold more haloperidol was added to the SLN formulation (50 mg) than to the PLGA formulation (3.5 mg). Then after the 80% release, SLN still remains with 10 mg of the drug (20% of the SLN total cargo) to be sustained released, which is still higher than the PLGA formulation.

Remarkably, the SLN formulation was able to increase haloperidol AUC in the brain by 3.5-fold and 4.7-fold compared to free drug intranasal and IV, respectively; increased Tmax in the brain by 2-fold compared to IV; increased Cmax in the brain by 3.6-fold and 4.3-fold compared to free drug intranasal and IV; and increased MRT of the drug in the brain by 1.4-fold and 1.2-fold compared to free drug intranasal and IV.

Perphenazine

Perphenazine presents low aqueous solubility (<0.1mg/mL) and low bioavailability (30%-50%) due to is first pass metabolism in the liver.[77,89] To overcome this drawback, PLGA polymeric nanoparticles[77] and chitosan-dextran sulfate (Chi-DS) nanoparticles[89] nano-DDSs were developed for perphenazine delivery. The Chi-DS nanoparticles presented a higher encapsulation efficiency of the perphenazine drug load (from 73% to 89% of the drug load for Chi-DS compared to 39.9% to 71.6% of the drug load for PLGA nanoparticles). Both systems presented an initial burst release of the drug followed by a sustained release pattern (~80% of the drug load within the first 20 h and ~70% of the drug load within the first 8 h for PLGA and Chi-DS nanoparticles, respectively). Interestingly, increasing the amount of PLGA also decreased the burst release effect (>60% of the drug load within first 20 h), which indicates some problem in solvating the drug into the polymer matrix, as discussed in the chlorpromazine section before. Regarding the Chi-DS nanoparticles, the authors argue that this burst release was driven by weakened electrostatic forces that held perphenazine to the dextran sulfate nanoparticle surface. Thus, better solvation of the drug into the chitosan–dextran sulfate matrix may prevent the initial burst release, as the drug release would be relying more on diffusion than electrostatic forces.

Atypical antipsychotic delivery

Clozapine

Clozapine is the first and most prominent atypical antipsychotic.[78,93,94] However, it presents poor bioavailability (<27%[93]) due to extensive hepatic metabolism and extensive metabolic blood clearance/low plasma half-life,[83,94] thus requiring higher doses for therapeutic outcomes which can cause side effects.[78] To overcome these drawbacks, PLGA polymeric nanoparticles,[78] poly-(ε-caprolactone) (PCL) nanocapsules coated with either polysorbate 80, PEG or chitosan,[70] shell polymeric nanocapsules made of layers of PLGA and Poly-L-Lysine (PLL) with emulsion core[83,84] and (SLN) made of a triglyceride (trimyristin, tripalmitin or tristearin), phosphatidylcholine and poloxamer 188[93,94] were developed for clozapine delivery.

All of these nano-DDSs presented similar encapsulation efficiency (93.17% to 94.74% for PLGA, 68.0% to 95.8% for

Table 3
Nano-DDSs used for schizophrenia treatment.

Nano-DDS series	Nano-DDS type	Author, year and reference	Drug used	Average diameter (nm)	ζ-potential (mV)	PDI	Amount of drug incorporated (mg)
Polymeric nanoparticles	PLGA	Muthu et al, 2009[82]	Risperidone	84.1-219.1	NR	0.616-0.899	5 and 10
		Seju et al, 2011[80]	Olanzapine	91.2	−23.7	0.120	6.25
		Halayqa et al, 2014[77]	Chlorpromazine	374.3-476.7	NR	0.098-0.243	10
		Halayqa et al, 2014[77]	Perphenazine	325.5-419.1	NR	0.105-0.159	10
		Panda et al, 2016[78]	Clozapine	248.0-392.0	(−11.1)-(−13.5)	0.130-0.300	10
		Panda et al, 2016[78]	Risperidone	248.0-392.0	(−11.1)-(−13.5)	0.130-0.300	5
	PEG-PLGA	Piazza et al, 2014[79]	Haloperidol	121.0-132.0	(−11.1)-(−14.4)	0.149-0.174	3.5
	Poly-L-Lysine – PLGA	Lukasiewicz et al, 2016[83]	Clozapine	100.0	(−4)	<0.2	NR
		Lukasiewicz et al, 2017[84]	Clozapine	100.0	(−4)	NR	NR
	PCL	Muthu et al, 2008[85]	Risperidone	99.1-303.9	(−22.4)-(−29.7)	0.082-0.161	5
		Vieira et al, 2016[70]	Clozapine	64.0-233.7	(−33.2)-29.0	NR	15
		Sawant et al, 2016[86]	Aripiprazole	188.6-323.4	NR	NR	2
		Joseph et al, 2018[87]	Olanzapine	47.8-112.2	(−16.8)-(−35.6)	0.111-0.775	5, 15, 30

Entrapment efficiency (%)	*In vitro* drug release	*In vivo* dose (mg/kg)	AUC	Cmax	Tmax
86.6-95.1	Sustained release in phosphate buffer saline with the release of >80% of the drug load in 72 h	5 SC once	NR	NR	NR
68.9	Release of 90.2% of the drug load in phosphate buffer saline in the first 7 h	1.45 IN once	NR	Significantly different than IN and IV; 1.8-fold increase compared to IN free drug.	Significantly different than IN and IV; 1.3-fold increase compared to IN free drug.
44.8-71.0	60% to 90% of the drug load released in phosphate buffer saline during the first 8 h, followed by sustained release from 8 h to 48h.	NR	NR	NR	NR
39.9-83.9	60% to 80% of the drug load released in phosphate buffer saline with 24 h, followed by sustained release from 24 h to 100 h.	NR	NR	NR	NR
93.2-94.7	Sustained release of 80% of the drug load in phosphate buffer saline within the first 240 h	NR	NR	NR	NR
90.4-93.1	Sustained release of 82% of the drug load in phosphate buffer saline within the first 240 h	NR	NR	NR	NR
73.2-82.5	Sustained release of 7.4%-7.56% of the drug load in both acetate buffer and phosphate buffer saline +0.1% Tween 80 within 96 h	NR	NR	NR	NR
~100	NR	NR	NR	NR	NR
~100	NR	NR	NR	NR	NR
81.4-85.4	Release of 80% and 50% of the drug load in phosphate buffer saline within the first 2 h and 0.5 h, respectively.	5 IV daily for 3 days	NR	NR	NR
68.0-98.0	Release of 34.4%-47.7% of the drug load in phosphate buffer saline+ethanol (7:3) within the first 12 h	5 IP once	Significantly different; 2.7-fold increase compared to free drug	Significantly different; 4.3-fold increase compared to free drug	Not significantly different than free drug
42.4-69.8	Sustained released of 89.5% of the drug load in phosphate buffer saline +5% SLS within the first 72 h	40 IP once	No comparison with the free drug	No comparison with the free drug	No comparison with the free drug
61.6-82.6	Sustained release of >80% of the drug	10 IV	Significantly different; 1.2-fold and 1.7-fold	Significantly different; 1.4-fold and 2.4-fold	Significantly different; 2-fold increase

Nano-DDS series	Nano-DDS type	Author, year and reference	Drug used	Average diameter (nm)	ζ-potential (mV)	PDI	Amount of drug incorporated (mg)
	PLGA-PCL-PVA	Alzubaidi et al, 2017[88]	Risperidone	201-1358	NR	NR	50
	Chitosan-dextran sulfate	Dong and Hadinoto, 2017[89]	Perphenazine	80.0-100.0	(−50)-(−70)	0.54	5
	Chitosan-TPP	Ruby and Pandey, 2016[90]	Olanzapine	183.1	52.1	0.122	20
		Shah et al, 2016[71]	Quetiapine	140.1-487.5	34.4	0.239-0.478	NR
	Polymeric micelles	Patil et al, 2018.[91]	Aripiprazole	167.8-236.4	(−3.32)-(−11.2)	0.211-0.339	30
Lipid nanoparticles	Liposome	Narayan, 2016[92]	Risperidone	91.9-209.0	(−52.2)-22.4	NR	NR
	SLN	Venkatesarlu & Manjunath, 2004[93]	Clozapine	96.7-266.3	0.2-33.2	NR	40
		Manjunath & Venkatesarlu, 2005[94]	Clozapine	96.7-233.3	0.2-33.2	0.146-0.386	40
		Sood et al, 2013[95]	Olanzapine	311.9-404.6	1.87-33.2	NR	5 and 10
		Kumar and Radhawa, 2013[96]	Paliperidone	267.0-328.0	(−50.3)-(−45.3)	NR	50
		Narala and veerabrahma, 2013[72]	Quetiapine	167.8-271.8	(−18.5)-(−28.1)	0.230-0.441	10
		Shikha et al, 2013[73]	Quetiapine	93.6-157.4	NR	0.201-0.342	5-20

Entrapment efficiency (%)	*In vitro* drug release	*In vivo* dose (mg/kg)	AUC	Cmax	Tmax
	load released in phosphate buffer saline +2% Tween 80 within the first 60 h		increase compared to the free drug	increase compared to the free drug	compared to the free drug
61.0-83.3	Sustained release of 26.2% to 82.5% of the drug load in phosphate buffer saline within the first 24 h	0.3 OF once	Significantly different; 1.9-fold increase compared to the commercial formula (Risperidal®)	Significantly lower than commercial formula (Risperidal®) (30% lower)	Significantly different; 2.3-fold increase compared to the commercial formula (Risperidal®)
60.0-80.0	Release of 40%-70% of the drug load in phosphate buffer saline within the first 8 h	NR	NR	NR	NR
72.4	Release of 21%-42% of the drug load in phosphate buffer saline +methanol (7:3) within the first 5 h	NR	NR	NR	NR
68.1-92.3	Release of >60% of the drug load in phosphate buffer saline within the first 12 h	2.3 IN once	Significantly different; from 1.7-fold and 2.1-fold increase compared to free drug in the blood and in the brain, respectively	Significantly different; from 1.3-fold and 2.6-fold increase compared to free drug in the blood and in the brain, respectively	Not significantly different than free drug in the blood and in the brain
74.5-79.2	Release of 97.4% of the drug load in phosphate buffer saline +1% SLS within the first 20 h	NR	NR	NR	NR
30.2-58.9	Release of 40.2%-57.0% of the drug load in phosphate buffer saline within the first 4 h	0.36 IV once	Significantly different; from 1.4-fold to1.6-fold increase compared to free drug	Significantly lower than free drug (40% lower)	Significantly different; 6-fold increase compared to free drug
93.4-98.8	Release of 17.7%-51.0% of the drug load in phosphate buffer saline, 0.1 N HCl or distilled water within the first 48 h	NR	NR	NR	NR
93.6-98.8	NR	10 IV; 20 ID both once	Significantly different for both IV and ID; 1.5-fold to 4.5-fold increase compared to free drug	Significantly different; 3.2- to 4.2-fold increase compared to free drug	Significantly different; 1.3- to 2-fold decrease compared to free drug
11.1-63.4	Sustained release of 95.7% and 62.0% of the drug load in phosphate buffer saline +1% methanol within the first 48 h	9 OF once	Significantly different; 4-fold increase compared to free drug	Significantly different; 2.9-fold increase compared to free drug	Significantly different; 4.9-fold increase compared to free drug
55	NR	NR	NR	NR	NR
82.4-92.1	Sustained released of 50%-75% of the drug load released in phosphate buffer saline within the first 24 h	10 OF once	Significantly different; 3.7-fold increase compared to free drug	Significantly different; 17.8-fold increase compared to free drug	Not Significantly different than free drug
36.1-81.3	Release of 93.7 to 97.8 of the drug load in phosphate buffer saline within the first 8 h	4 IV once	Significantly different; 2-fold and 25.7-fold increase in the brain compared to free quetiapine fumarate and hemifumarate, respectively.	Significantly different; 1.7-fold and 3.7-fold increase in the brain compared to free quetiapine fumarate and hemifumarate, respectively.	Not Significantly different than both free drugs.

Nano-DDS series	Nano-DDS type	Author, year and reference	Drug used	Average diameter (nm)	ζ-potential (mV)	PDI	Amount of drug incorporated (mg)
		Kõumar and Radhawa, 2014[8]	Paliperidone	100.3-392.5	(−21.1)-(−19.4)	0.440-0.680	NR
		Yasir et al, 2014[97]	Haloperidol	115.1-156.8	(−13.7)-(−16.7)	0.409-0.479	43.75 and 50
		Aboti et al, 2014[74]	Quetiapine	176.7-820.4	8.13	0.228-0.698	NR
		Kumar and Radhawa, 2015[98]	Paliperidone	200-1700	NR	0.390-0.430	NR
		Joseph et al, 2017[99]	Olanzapine	146.0-346.0	(−28.4)-(−38.8)	0.305-0.588	NR
		Natarajan et al, 2017[100]	Olanzapine	110.5-165.1	35.3-66.5	0.340-0.742	5
		Gambhire et al, 2018[101]	Asenapine	143.0-258.0	NR	NR	NR
	NLC	Mandpe et al, 2013[102]	Iloperidone	59.2	NR	NR	NR
	Glycol chitosan-NLC	Singh et al, 2017.[103]	Asenapine	167.3-187.0	(−4.3)-18.9	NR	80
	Self nano-emulsifying	Miao et al, 2015[75]	Lurasidone	62.4-67.3	(−22.1)-(−25.5)	0.123-0.147	40
		Dondapati et al, 2016[104]	Lurasidone	126.9-309.1	NR	0.222-0.687	5
		Miao et al, 2016[12]	Ziprasidone	54.5-62.3	-28.0	NR	20

Entrapment efficiency (%)	*In vitro* drug release	*In vivo* dose (mg/kg)	AUC	Cmax	Tmax
75	NR	NR	NR	NR	NR
68.4-71.6	Sustained release of >80% of the drug load released in phosphate buffer saline within the first 96 h	0.89 IN once	Significantly different; 3.5-fold and 4.7-fold increase in the brain compared to free drug IN and IV	Significantly different; 3.6-fold and 4.3-fold increase in the brain compared to free drug IN and IV	Significantly different compared to IV, but not significant different than IN; 2-fold increase in the brain compared to IV
60.1	Release of 80% of the drug load in phosphate buffer saline within the first 12 h	10 OF once	Significantly different; 10-fold increase compared to the free drug	Significantly different; 5-fold increase compared to free drug	Not significantly different than free drug
NR	Sustained release of ~50% of the drug load in phosphate buffer saline or 0.1 N HCl after 48 h	NR	NR	NR	NR
50.5-88.9	Sustained release of >80% of the drug load in phosphate buffer saline + 2% Tween 80 within the first 48 h	3 IV daily for 28 days	Significantly higher than free drug	NR	NR
67.2-96.3	Sustained release of 30% and 70% of the drug load in phosphate buffer saline within 48 h	0.9 IV once	Significantly different; 1.9-fold increase in the blood and 38-fold increase in the brain compared to free drug	significantly different in the blood in the brain; increase of 2.2-fold in the blood and >10-fold in the brain compared to free drug	Significantly different in the blood but not in the brain; 2-fold in the blood compared to free drug IN and IV
70.7-80.5	Sustained release of ~70% of the drug load in phosphate buffer saline within the first 24 h	30 OF once	Significantly different; 6-fold increase compared to the free drug via IN in the blood	Significantly different; 1.8-fold increase compared to the free drug via IN in the blood	Significantly different; 2-fold increase compared to the free drug via IN in the blood
96.3	NR	1 IV and IN once	Significantly different; 3.1-fold increase compared to the free drug via IN	NR	NR
83.4-83.5	Sustained release of 80% of the drug load in phosphate buffer saline within 24 h	1 IN once	Significantly different; 2.4-fold increase compared to the free drug via IN in the blood and 4-fold increase compared to the free drug via IN in the brain	Significantly different; 1.3-fold increase compared to the free drug via IN in the blood and 1.8-fold increase compared to the free drug via IN in the brain	Significantly different; 3-fold increase compared to the free drug via IN in the blood but not in the brain.
99.9%	Release of >90% of the drug load in phosphate buffer saline within the first 5 min	134 OF once	Significantly different than Latuda®; 1.3-fold and 2.7-fold increase compared to fed and fasting dogs, respectively.	Significantly different than Latuda®; 1.2-fold and 2.7-fold increase compared to fed and fasting dogs, respectively.	Not significantly different than Latuda® in both fed and fasting dogs.
97.0%-98.3%	Release of >70% of the drug load in phosphate buffer saline within the first 10 min	NR	NR	NR	NR
99.9	Release of >90% of the drug load in water, 0.1 N HCl or phosphate buffer saline within the first 1.5 h	2 OF once	Significantly different than Zeldox®; 1.6-fold and 2.8-fold increase compared to fed and fasting dogs, respectively.	Significantly different than Zeldox®; 1.3-fold increase compared fasting dogs but not significantly different than Zeldox® in fed dogs.	Significantly different than Zeldox®; 2.4-fold and 3-fold increase compared to fed and fasting dogs, respectively.

Nano-DDS series	Nano-DDS type	Author, year and reference	Drug used	Average diameter (nm)	ζ-potential (mV)	PDI	Amount of drug incorporated (mg)
Nanocrystal	Lurasidone nanocrystal	Shah et al, 2016[105]	Lurasidone	228	NR	NR	5
Hybrid nanoparticles	Lipid-polymer	Helal et al, 2017[106]	Paliperidone	156.0-258.0	(−34.2)-(−13.1)	0.200-0.310	3

PCL and 89.7 to 97.2% for SLN). PLGA and SLN presented a similar sustained release profile (from 18% to 38% of the drug load within the first 3 days followed by a sustained release of the drug up to 54% to 80% within the next 7 days, depending on the polymer viscosity for PLGA, while SLN released 15.32% to 50.92% of its cargo in 48 h depending on the triglyceride and the amount of polomer 188 used). Differently from those, PCL nanoparticles presented a higher initial release of clozapine within the first 12 h (from 34.4% to 47.7% of the load). Interestingly, the PLGA and poly-L-lysine (PLL) with 2 layers showed no diffusion resistance to clozapine release. However, increasing the layers also increased the clozapine release resistance, indicating a reduction of the nanoparticle porosity due to the increased layers.

Further studying these formulations *in vivo*, nano-DDSs demonstrated a remarkable increase of clozapine Cmax,[78,88] AUC,[70,94] elimination half-life[78,88] and MRT[78,88] compared to the free drug. Interestingly, one study was able to decrease Tmax by 1.3- and 2-fold,[94] which could decrease of the dose available outside of the SLN for tissue absorption, thus decreasing the Tmax. This could be related to the in vitro release of the drug by the chosen nanoparticle, which released ~50% of the drug load after 48 h.[93]

Regarding the ability of the PLGA and PLL nanoshell on crossing the blood–brain barrier (BBB), Lukasiewicz et al[84] used hCMEC/D3 cell line to mimic the BBB. The authors demonstrated that transcytosis was the main mechanism for crossing the BBB. Amusingly, the nanoparticle formulation presented an 8-fold increase in crossing the BBB related to the clozapine-free. thus indicating that the nano-DDS would effectively increase clozapine brain absorption once it reaches the BBB.

Olanzapine

Olanzapine presents high volume of distribution (~1000 L) and extensive hepatic first-pass metabolism via cytochrome P450, in a such degree that only a fraction of the drug reaches its target tissue. Thus, to be effective, higher doses of olanzapine are required, consequently, promoting side effects to the patient.

Regarding the lipid nanoparticles, Joseph et al[99] developed two solid lipid nanoparticles formulations (coated with polysorbate 80 or not) for olanzapine delivery by homogenization–ultrasonication technique (Figure 9). Interestingly, the coated nanoparticles were able to encapsulate similar olanzapine than the uncoated (72.96 % and 74.51%, respectively), which could indicate that olanzapine was solubilized into the lipid core of the nanoparticle and not bound to its surface. Possibly, due to this, both formulations presented a controlled release pattern up to 48 h when compared to the free drug.

Similarly, Natarajan et al[100] and Sood et al[95] developed two SLN formulations for olanzapine delivery. Natarajan et al produced SLN using glyceryl monostearate (GMS) or glyceryl tripalmitate (GTP), While Sood et al produced SLN containing Glyceryl monostearate (GMS) or stearic acid (SA). We can see that SA entrapped less olanzapine than GMS-SLN, which entrapped even less olanzapine than GTP-SLN (30% of olanzapine entrapment for SA, 62.7%-70% for GMS, and 96.3% for GTP). These differences could be due to the physical structure of the involved lipids inside of the lipid core. GTP contains three aliphatic carbon chains linked together by the glyceryl moiety, while GMS and SA contain only an aliphatic carbon chain. Because of this, GTP molecules would promote a less ordered core / bigger imperfections inside of SLN core than GMS and SA, thus opening space for olanzapine incorporation among the fatty acids. By these data, it is possible to infer that the glyceryl moiety inside of the GMS molecules would promote even a less ordered core / bigger imperfections inside of SLN core than SA.

Interestingly, these SLN inner core imperfections seem to also impact the release of olanzapine load between GTP and GMS, as 70% of the drug load was released in 48 h for GMS-SLN, while GTP-SLN released only 30% of the drug load in the same period. While no apparent differences were found between SA and GMS. Regarding polymeric nanoparticles, all formulations presented similar encapsulation efficiency (76.92% and 78.77%, 72.42% and 69.78%, respectively). All formulations presented a sustained release pattern, by releasing olanzapine load up to 120 h when compared to the free drug.

Regarding the *in vivo* tests, nano-DDSs formulations increased AUC,[87,95,99,100] Cmax,[80,87,95,100] Tmax[80,87,95,100] and MRT[87,95,100] compared to free olanzapine. Amusingly, the

Entrapment efficiency (%)	*In vitro* drug release	*In vivo* dose (mg/kg)	AUC	Cmax	Tmax
NR	Release of >75% and 49.3% of the drug load in phosphate buffer saline within 10 and 2 min, respectively	NR	NR	NR	NR
87.2	Sustained release of ~60% of the drug load in phosphate buffer saline within 24 h	NR	NR	NR	NR

GTP-SLN formulation of Natarajan et al[100] presented a 38-fold increase of olanzapine AUC in the brain compared to the free drug in 24 h.

Remarkably, nano-DDSs significantly inhibited olanzapine body-weight gain compared to free drug from day 10 to day 28[99] and catalepsy score up to 240 min after the injection[87] compared

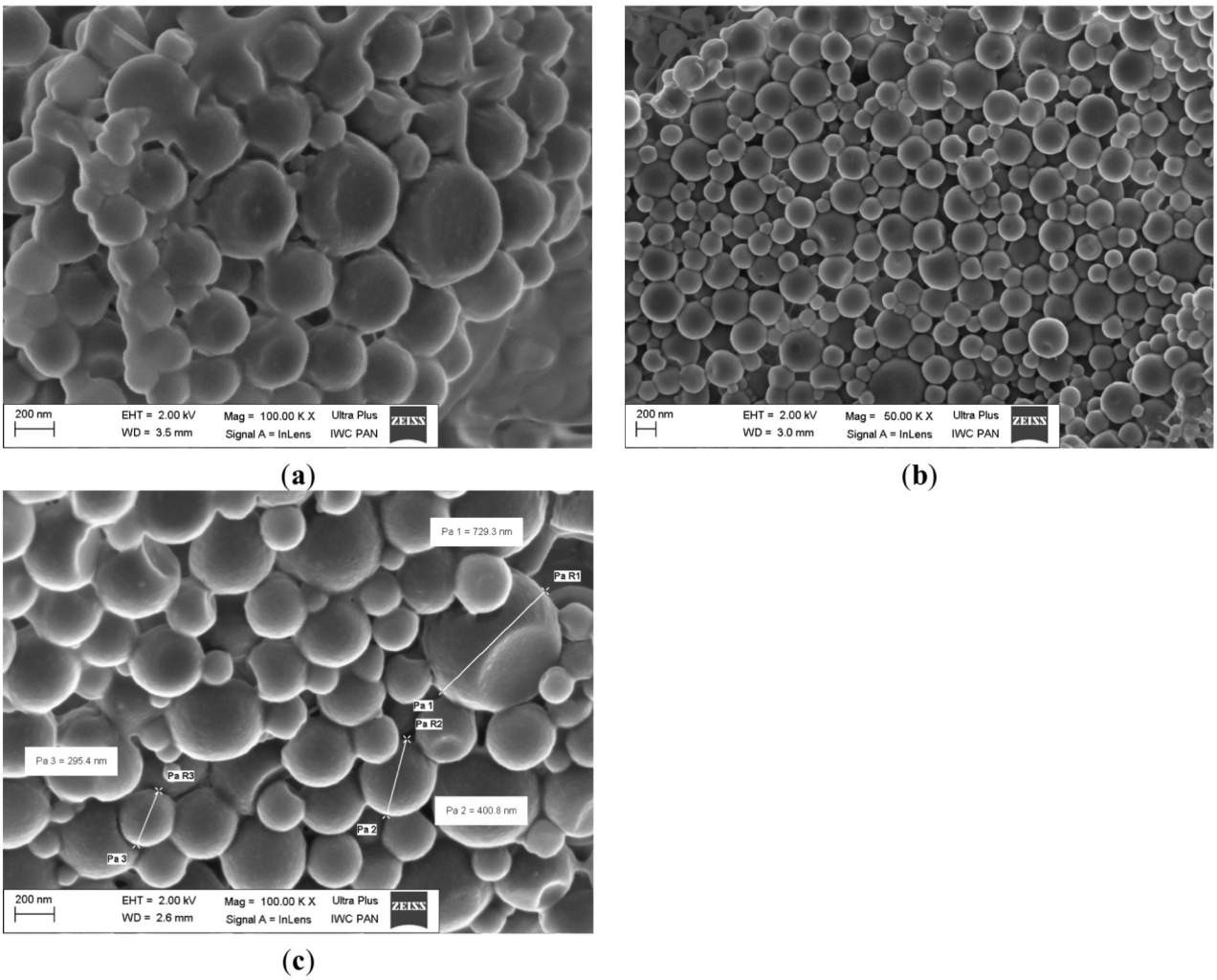

Figure 8. Scanning electron microscopy (SEM) of chlorpromazine-loaded PLGA nano-DDS prepared with PLGA concentration at **(A)** 0.8% (w/v); **(B)** 1.3% (w/v); **(C)** 1.6% (w/v) at TDL 20% (w/w). Reproduced from Halayqa et al.[77]

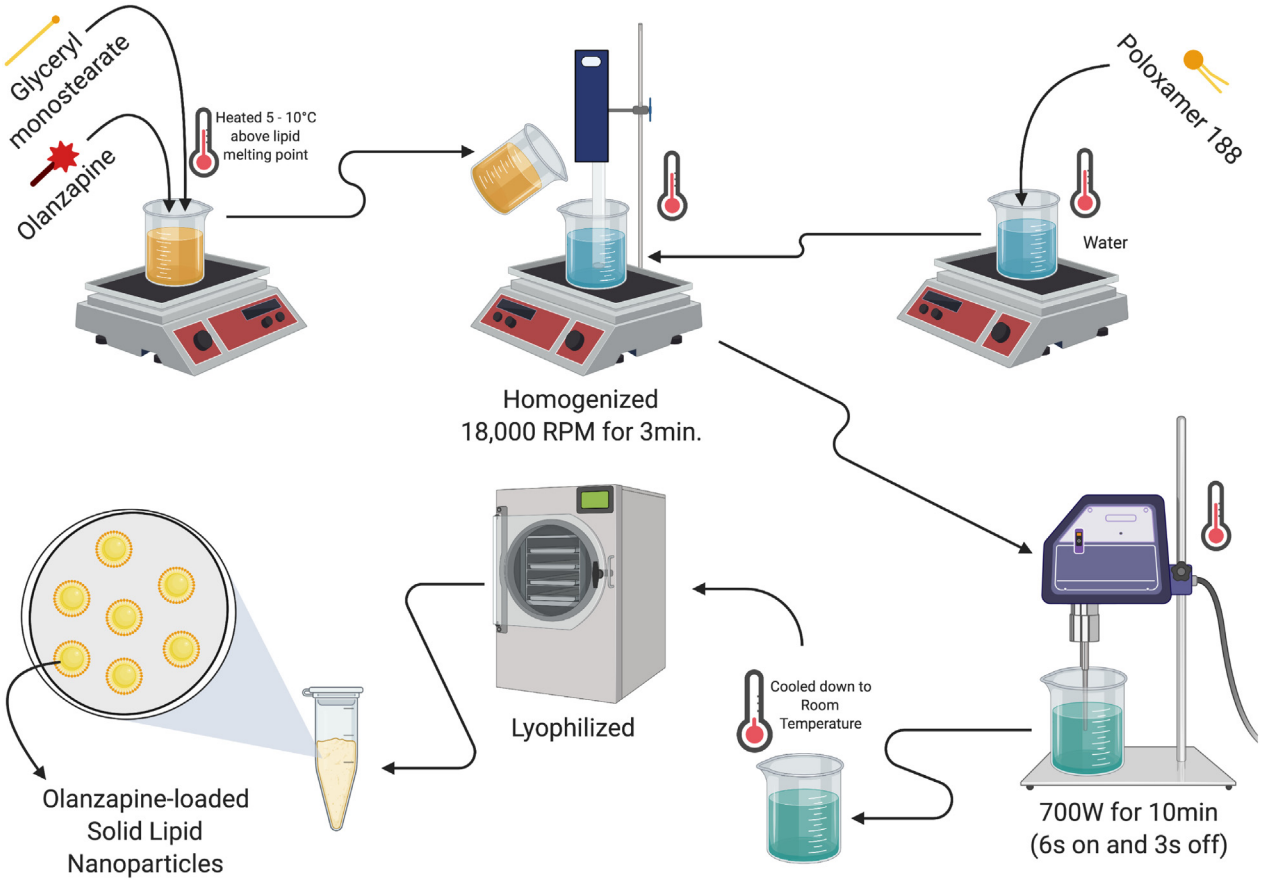

Figure 9. Synthesis of olanzapine-loaded solid lipid nanoparticle (SLN), as described by Joseph et al.[99] Created with BioRender.

to the free drug *in vivo*. Outstandingly, nano-DDSs significantly inhibited apomorphine-induced psychosis behavior from 0.5 to 24 h after the apomorphine injection, while the free drug inhibited only up to 8 h.[99]

Iloperidone

Iloperidone is extensively metabolized and its main metabolite (P88) has comparable efficacy to the parent drug and is also able to cross the blood–brain barrier.[112] To overcome this drawback, a nanostructured lipid carrier (NLC) formulation[102] was developed for iloperidone delivery. Remarkably, NLC presented an encapsulation efficiency of 96.25% and, after being administered intranasally (1 mg/kg of iloperidone) in male Wistar rats, the nano-DDS formulation obtained a 3-fold increase of the *in vivo* AUC and 2-fold increase of targeting efficiency into the brain, compared to the free drug.

Lurasidone

Lurasidone has very low aqueous solubility (0.224 mg/ml at 20 °C) and high plasma protein-binding (99.8%) independent of the concentration and presents significant food-effect on the bioavailability of the drug.[113] All of these factors contribute can be responsible for low bioavailability of the drug (~9% to 19% of the administrated mass).[105,113] To overcome these drawbacks, a lurasidone hydrochloride nanocrystal stabilized with hydroxypropyl-methyl-cellulose[105] and self-emulsifying formulation[75,104] were developed for lurasidone delivery.

Although these formulations presented a high entrapment efficiency of the drug (>90%), most of the drug load (>95%) was burst released within the first 5 to 60 min. As for other lipid nanoparticles, the self-emulsifying formulation burst release could be indicative of a poor entrapment of the drug load in the lipid matrix. However, as both studies demonstrated that the chosen oils (caprylic/capric glycerides (Capmul MCM) and anise oil) have higher lurasidone solubility compared to other tested oils, another explanation should be displayed. Possibly, both of these oils present a very rigid liquid-crystal structure when emulsified, thus not letting enough imperfections for drug incorporation and releasing the drug load within the first hour. Regarding the nanocrystal formulation, it was the authors' objective to release >85% of the lurasidone load within the first 5 min to improve the saturation solubility of the drug. This objective was achieved, as only ~25% of free lurasidone was present in the dissolution media after 60 min, while the nanocrystal formulation released >80% of the drug in the dissolution media in less than 10 min. However, this approach (releasing most of the drug within the first 5 min) might not be suitable for therapeutic purposes, as lurasidone presents a high plasma protein binding (99.8%) independent of concentration. Regarding this lurasidone issue, an ideal approach would be to

specifically protect the drug from plasma binding, cross the BBB and only release the lurasidone load in the target tissue, i.e. the brain. In this context, lower concentrations of the drug than what is traditionally used in schizophrenia therapy would be necessary to take effect.

Amazingly, Miao et al[75] demonstrated that the nano-DDS formulation increased lurasidone AUC and Cmax of lurasidone up to 2.7-fold compared to commercial formulation (Latuda®). Also, they demonstrated that the nano-DDS pharmacokinetics was independent of fasting or feeding, while Latuda® demonstrated a decrease of the pharmacokinetics parameters during fasting.

Risperidone

Risperidone is practically insoluble in water and undergoes significant first-pass metabolism, leading to low bioavailability and plasma half-life (~3 h).[85] To overcome these drawbacks, PLGA,[78,82] PCL,[85] a mixture of PGLA, PCL, and poly-vinyl alcohol (PVA)[88] and liposomal[92] formulations were developed for risperidone delivery.

Higher encapsulation efficiency was found for polymeric nanoparticles compared to the liposomal formulation regarding risperidone delivery. The PLGA formulations ranged from 86.6% to 95.10%; the PCL formulations ranged from 81.4% to 85.4%, while the liposomal formulation ranged from 29.46% to 49.60%. Even the polymer mixture formulations presented higher encapsulation efficiency (59.02% to 83.30%) than the liposomal formulation.

Regarding drug release, one PLGA nano-DDS formulation released 19% to 34% of the drug load within the first 3 days followed by a gradual release of the drug up to 54% to 82% within the next 7 days,[78] while the other formulations (another PLGA,[82] PCL[85] and liposomal[92] nano-DDS formulations) burst released 40%-60% of the drug content within the first 2 to 4 h. Interestingly, only the second PLGA formulation demonstrated a controlled release profile (releasing from 71% to 97% of the drug load) within the first 24 h.[82] For comparison, 80% to 90% of free risperidone has been found in the dissolution media in the first 2 h to 4 h.[82,85] Intriguingly, considerably different release pattern was found even within the same nanoparticle matrix. This different release pattern, though, may be due to different PLGA viscosity of the nanoparticles when produced by different methods (spray drying[78] vs. nanoprecipitation method[82]). A more viscous polymer may be formed by the spray drying process, limiting the drug motility and retarding risperidone release.

Although the PCL formulation demonstrated an encapsulation efficiency compared to the spray drying PLGA formulation, the release pattern was also very different, which could be due to different risperidone solvation efficiency in both polymeric matrixes and a viscosity closer to the nanoprecipitation PLGA formulation, thus burst releasing the drug.

Regarding *in vivo* experiments, two nano-DDSs (i.e. PLGA-PCL-PVA nano-DDS formulation[88] and lipossome[92]) were able to increase the AUC and Tmax of risperidone up to 1.9-fold and 6-fold in rabbit serum and Wistar rats, respectively. Remarkably, two nano-DDS formulations (i.e. PLGA[82] and PCL[85] formulations) were able to significantly reduce the catalepsy score in Wistar rats in the first 4 h and 8 h after subcutaneous injection and for 4 h, 8 h and 12 h in Swiss albino mice. Also, the PCL formulations were able to significantly reduce apomorphine-induced psychosis in Swiss albino mice up to 72 h compared to control, while the free drug was able to inhibit the apomorphine-induced psychosis up to 8 h.

Paliperidone

Risperidone principal metabolite (9-hydroxy risperidone, also known as paliperidone) still possesses therapeutic capabilities to treat schizophrenia.[85] However, paliperidone is practically insoluble and has low partition coefficient, thus leading to low oral bioavailability (28%[106]) and difficulty to cross the blood–brain barrier.[96,106] To overcome these drawbacks, newer paliperidone nano-DDS formulations are still being developed, i.e. SLN[8,96,98] and a lipid-polymer hybrid.[106]

The SLN formulations presented 42.4% and 55% of drug entrapment efficiency depending on the solid lipid (stearic acid[98] and containing glycerol stearate (Capmul GMS 50K),[96] respectively). The authors argue that the lower entrapment efficiency of the stearic formulation compared to the Capmul GMS 50K was due to a higher crystallinity of the stearic acid compared to Capmul GMS 50k. Fascinatingly, the addition of Gelucire® 50/13, a glyceride of PEG-ester and a fatty acid, increased the entrapment efficiency from 55% to 75%.[8]

Interestingly, the lipid-polymer hybrid nanoparticles was composed of PCL for polymeric core, a lipid coat made of Lipoid S75 and Gelucire® 50/13 and stabilized by polyvinyl alcohol (PVA).[106] The optimized nanoparticle presented 87.27% of drug entrapment efficiency and a 24 h controlled release pattern. Remarkably, the hybrid formulation increased the intestinal permeation flux compared to the free drug.

Aripiprazole

Although aripiprazole has good oral bioavailability (up to 87%), it undergoes extensive first pass metabolism (both hepatic and P-glycoprotein efflux metabolisms), leading to increased dose related side effects.[86,91] To overcome this drawback, a PCL polymer nano-DDS[86] and a polymeric micelles[91] nano-DDS were developed for aripiprazole delivery.

The polymer nano-DDS presented a slightly higher encapsulation efficiency compared to the polymeric micelles (87.27% compared to 74.53%-79.24%, respectively), while the PCL system presented a sustained release pattern; the polymeric micelles system burst released the drug, with 97.37% of the drug load released within the first 20 h.

Remarkably, the PCL nano-DDS intranasal delivery increased *in vivo* aripiprazole Cmax and drug distribution in the brain, and increased aripiprazole total plasma concentration AUC by 2-fold in male Sprague–Dawley rats compared to intravenous delivery of the nano-DDS.

Asenapine

Asenapine is a novel atypical antipsychotic drug (approved by USFDA and EMA in 2009 and 2011, respectively). However, it presents low bioavailability (~35% via sublingual and <2% via oral administration) due to its high first pass metabolism and presents a high food effect.[103] To overcome these drawbacks, an SLN[101] and glycol chitosan (GC) surface-modified NLC[103] nano-DDSs were developed to asenapine delivery.

Both nano-DDSs demonstrated similar asenapine encapsulation efficiency, with NLC encapsulation efficiency being very slightly higher than SLN (from 70.73% to 80.45% for SLN and 82.46% to 84.24% for NLC). Interestingly, as discussed before, a higher encapsulation efficiency is expected from NLC, as it contains greater amounts of crystal imperfections due to the presence of oil in the solid core.[76]

Both nano-DDSs demonstrated similar controlled release patterns, by releasing from 50% to 70% of asenapine load within the first 12 h (for SLN and NLC, respectively) and 90% of the drug load within the first 24 h. These results are somewhat intriguing, as NLC formulation is expected to release lower amounts of asenapine compared to SLN formulations. However, one possible explanation might be related to the amount of oil added to the NLC formulation. Possibly, the amount of oil added (160 mg of oleic acid) may be so low in the NLC formulation that it does not create enough crystal imperfection and does not interfere in the release pattern of the nanoparticles, thus making it very slightly different than the SLN formulation.

Remarkably, SLN formulation increased asenapine AUC by 5-fold, while GC-modified NLC increased 2.3-fold the AUC both compared to the free drug. SLN formulation also increased Cmax by 2-fold and both formulations increased the amount of asenapine in the brain, reaching up to 4-fold for the NLC formulation and 3-fold for the SLN formulation, both compared to free drug.

Since asenapine possesses inherent dose-dependent teratogenic potential, asenapine-loaded GC-modified NLC and the free drug were tested for fetal birth defects in Charles-Foster rats.[103] Remarkably, the nano-DDSs decreased the number of fetal birth defects 3-fold when compared to the free drug.

Quetiapine

Quetiapine fumarate presents a low plasma half-life (~6 h) and poor oral bioavailability (9%) due to first-pass metabolism.[72] To overcome these drawbacks, SLN[72–74] and chitosan/TPP[71] nano-DDSs were developed.

The SLN entrapment efficiency ranged considerably, from 1.76%[74] to 92.06%[72] of the drug load. This may be due to different composition of the produced SLN and different drug loads. The chitosan/TPP polymeric nano-DDS ranged from 64.88% to 92.26% of the drug load.

The release pattern also considerably ranged throughout the SLN studies, from releasing up to ~95% of the drug load in 8 h to releasing 71.2% in 24 h. Intriguingly, different free quetiapine releases were found. While Narala et al[72] describe that 75% of the free drug was released within the first 24 h, Aboti et al[74] describe 100% of free quetiapine release within the first 12 h. These different release patterns from the same free compound may be due to different amounts of quetiapine used in these tests or even differences in the dissolution methods. On the other hand, the polymeric nano-DDS was tested using ex-vivo nasal diffusion from these tests; the chitosan/TPP was able to diffuse more quetiapine than the free drug (65% and 40%, respectively).

Regarding the in vivo pharmacokinetics parameters, all of the nano-DDSs were able to increase the AUC and C_{max} of quetiapine, but two formulations outperformed the others. The SLN formulation of Narala et al[72] was able to increase quetiapine Cmax by 17.8-fold and $T_{1/2}$ by 1.5-fold, while the nano-DDS of Shikha et al[73] increased quetiapine hemifumarate AUC outstandingly by 27.5-fold. Both of these results are very impressive by how much they could modulate the pharmacokinetics parameters of quetiapine.

Ziprasidone

Although ziprasidone presents good oral bioavailability even when administered with food (60%), it has a very low solubility (0.3 mg/ml in water).[12] To overcome this drawback, a self-nanoemulsifying[12] nano-DDS was developed.

The nano-DDS presented 99.9% of encapsulation efficiency of the drug load, 90% of which was released within the first 12 h. Remarkably, the nano-DDS was able to increase 4.5-fold the *in vitro* release of the drug compared to the free drug. Also, the nano-DDS increased the drugs Tmax by 2.4-fold, MRT by 2-fold and AUC by 2.8-fold in fasted dogs compared to ziprasidone commercial formulation (Zeldox®). Interestingly, the nano-DDS Cmax for fed dogs was not significantly different from the commercial formulation. On the other hand, the self-nanoemulsifying formulation presented no food effect, while the commercial formulation decreased its *in vivo* pharmacokinetics parameters by 2-fold compared to fasting dogs.

Alternative treatments

Although nanopsychiatry can assist to turn the schizophrenia traditional treatments to be more effective, it can also be used to give rise to alternative treatment for schizophrenia, which, for instance could also solve the EPSE problem of the traditional treatments. The most prominent alternative schizophrenia treatment is through the endocannabinoid system. Briefly, the endocannabinoid system comprises of 2 cannabinoid receptors (CB1 and CB2); 2 endocannabinoids (Anandamine and 2-arachidonoylglyerol) which serves as ligand to the system; and enzymes involved in transportation, biosynthesis and metabolism of these endocannabinoids.[114,115] Anandamide is one of the main endocannabinoids acting on CB1 and CB2 receptors and is usually synthesized on demand.[115,116] Cannabinoid drugs that can interfere in the endocannabinoid system are being tested for treatment of several diseases, from cancer to neurological disorders, such as schizophrenia.[117,118] In the case for schizophrenia, clinical studies have shown that schizophrenia patients present abnormalities in the endocannabinoid system (i.e. increase of CB1 in several regions of the brain and increased levels of anandamide in the cerebrospinal fluid, when compared to normal tissues and fluids).[119] Therefore, targeting the endocannabinoid system is an alternative for the classical treatment of schizophrenia. However, clinical use of cannabinoid drugs is limited due to its unfavorable physical–chemical characteristics. In this sense, nano-DDS can be used to promote these drugs into the clinic by delivering these drugs into the target tissue.

Here, we divided the use of nano-DDS into delivery of agonists and antagonists of the endocannabinoid system.

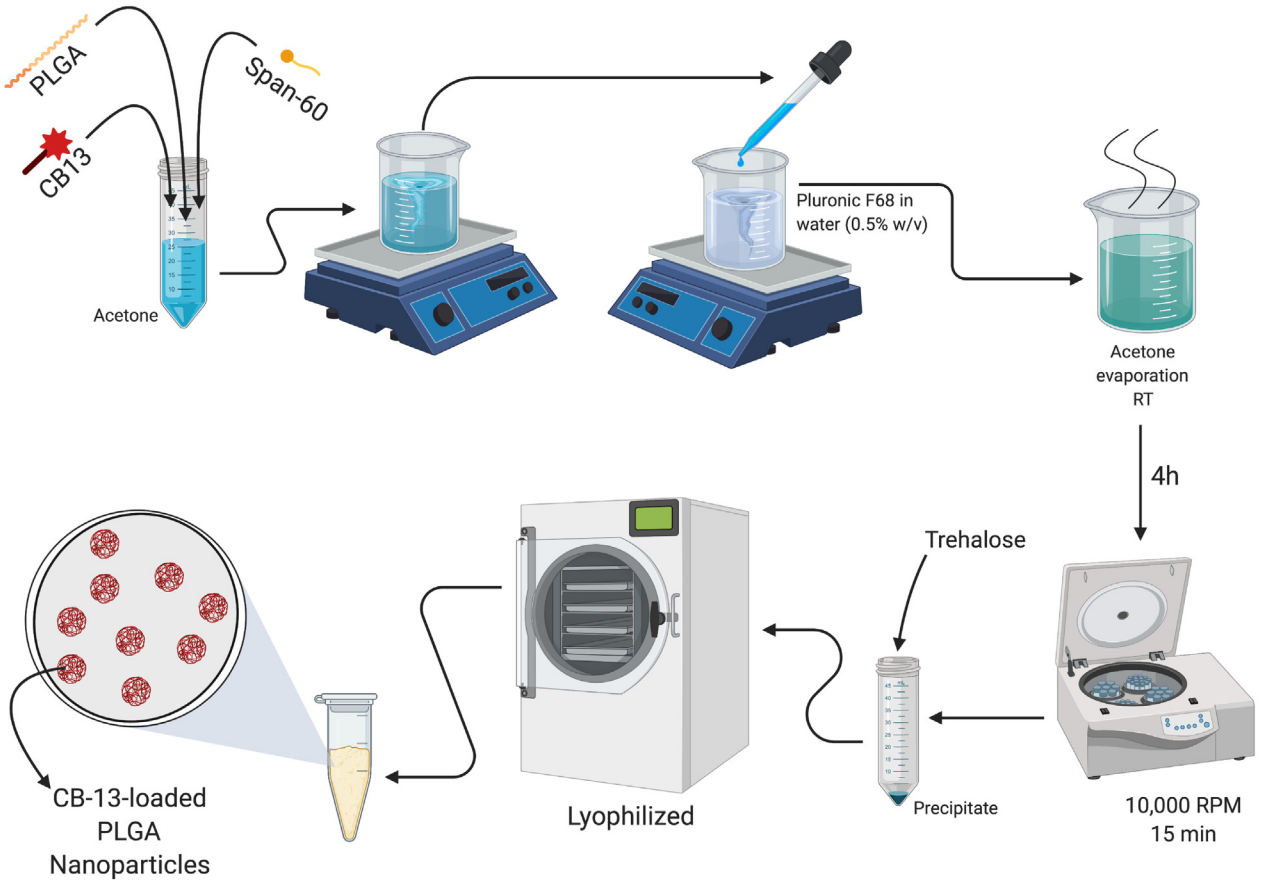

Figure 10. Synthesis of CB-13-loaded solid lipid nanoparticle (SLN), as described by Durán-Lobato.[124] Created with BioRender.

Delivery of endocannabinoid agonists

The synthetic cannabinoid receptor agonist 13 (CB-13) is a cannabinoid receptor agonist, with high affinity and functional activity to both CB-1 and CB-2 receptors.[120,121]

Durán-Lobato produced a series of research articles using different nano-DDSs for oral delivery of CB-13. The authors used plain-lipid nanoparticle[122]; chitosan- and PEG-coated polymeric PLGA and lipid nanoparticles[123] and plain-PLGA nanocarrier.[123,124]

On their first research article,[124] the authors demonstrate delivery of CB-13 to Caco-2 cells and CD/57 male mice using chitosan-, Eudragit® RS-, lecithin- and vitamin E-surface-modified poly(lactic-co-glycolic acid) (PLGA) nanoparticles. The synthesis method is shown in Figure 10. All the nanoparticles presented a yield of entrapment efficiency between 71% and 85.5%. Similar results (68% to 90%) were found for not-modified PLGA nanoparticles produced by Martín-Banderas formulated to carry the same drug. Both authors[123,125] argue that the high entrapment efficiency is due to the high octanol-water partition of CB-13, leading to an increased entrapment into the nanoparticle matrixes. The release of CB-13 was found to be between 35% and 90% after 15 days, which seems to be associated to diffusion and degradation/erosion mechanisms of drug release. The least sustained release nanoparticle was the lecithin-surface-modified PLGA nanoparticle, while the highest sustained release nanoparticle was the Eudragit® RS-surface-modified PLGA nanoparticles. The authors argue that this effect was due to Eudragit® RS as it has a low water permeability, which could produce a waterproof matrix hindering the entrance of water and acting as a barrier against further drug diffusion into the bulk water. No cytotoxicity was found for all formulation up to 30 μM of CB-13 in Caco-2 for 24 h and 48 h. Same results were found for Martín-Banderas for both normal (CCD-18Co) and metastatic colon (T84) cell lines for 24 h and 48 h. Interestingly, Durán-Lobato also shows free CB-13 showed cytotoxicity after 48 h. Durán-Lobato et al argue that this cytotoxic effect might be due to CB-13 anti-carcinogenic effect in Caco-2 cells, which are known to be a colon cancer cell line. Chitosan-surface-modified PLGA nanoparticles presented a significantly higher cellular uptake compared to all other nanoparticles. Finally, the authors demonstrated that surface-modifying the PLGA nanoparticles did not prevent the opsonization process, as most of the nanoparticles injected in vivo were found in the liver and in the spleen and less than 20% of the nanoparticles were found in the brain.

On their second research article,[123] Duran-Lobato et al studied the efficacy of coating PLGA and lipid nanoparticles with either chitosan or poly-ethylene-glycol (PEG). The formulations presented an entrapment efficiency between 73.4% and 91.3%. Regarding drug release, coated and not-

coated lipid nanoparticles released ~100% of CB-13 load in 6 h, while coated and not-coated polymeric nanoparticles released ~50% of the CB-13 load in 140 h. The authors used 0.1% (w/v) Tween 80 as dissolution medium to keep CB-13 sink conditions and, at certain time intervals filtered 500 μL of this solution to measure the amount of released CB-13. Detergents, like Tween 80, however, are able to disrupt the lipid nanoparticles, thus releasing the drug load. In this case, the addition of the detergent could impact the lipid nanoparticle release of CB-13 by promoting it to be earlier than without the detergent. Interestingly, chitosan-coated nano-DDS led to a higher interaction with Caco-2 cells and a limited uptake in THP1 macrophage cells, while PEG-coated nano-DDS led to a limited uptake in Caco-2 cells and strongly prevented THP1 macrophage cell uptake.

On their last research article,[122] Durán-Lobato et al developed lecithin-coated and uncoated lipid nanoparticle formulations to orally deliver CB-13. The formulations presented an entrapment efficiency between 70% and 100%. All formulations were stable after 2 months at 4 °C and 24 h in simulated intestinal conditions. However, under 24 h simulated gastric conditions, the uncoated nanoparticles got readily unstable by agglomeration. Previously, it has been demonstrated that lipid nanoparticles are stable for more than 3 years under 4 °C,[126,127] while PLGA nanoparticles seem to start degrading after 6 h at 4 °C.[125] Finally, all formulations were proved to be safe for use on mouse (3T3) and human (HEK293 and Caco-2) cell lines for 24 h.

Delivery of endocannabinoid antagonists

Although AM251,[128] rimonabant[129] and URB597[130] are considered as endocannabinoid antagonists, their mode of action is very different. While AM251 and rimonabant[129] act as selective CB-1 antagonist, URB597 is selective inhibitor of the fatty-acid amide hydrolase (FAAH), which catalyzes the intracellular hydrolysis of the endocannabinoid anandamide.[130] Rimonabant shows possible treatment of the emotional processing impairment presented in schizophrenic patients.[131] However, a 16-week clinical trial concluded that rimonabant did not improve global cognitive functioning but did improve a specific learning deficit based on response to positive feedback of schizophrenia patients.[132]

Esposito et al developed a nanostructured lipid carrier (NLC) formulation to deliver AM251, URB597 or rimonabant delivery to the brain. The authors were able to encapsulate from 92.8% to 99.9% of the drugs.[118] Focusing on the rimonabant delivery,[133] the authors show that 60% of the drug load was released from the nanoparticle between 20 and 25 h depending on the production method and the addition of polysorbate 80. Due to the low solubility of rimonabant in water, the authors used a non-physiological receptor phase with 30% v/v of ethanol to perform this assay. However, using ethanol in the receptor phase might be detrimental to the lipid nanoparticles, thus releasing the drug earlier than it would without ethanol. The brain–blood ratio is a convenient way for the estimation of brain pharmacokinetics and effectively evaluating the brain-targeting efficiency of neurotherapeutics.[134] Through this ratio, the authors remarkably show that rimonabant-loaded NLC was able to increase the brain-plasma ratio after intranasal administration in Sprague–Dawley rats when compared to free rimonabant.

Challenges

Adequate in vivo models

In this work, we demonstrate that nano-DDSs are able to significantly increase their psychoactive load into the blood and even in the brain. Since schizophrenia is a very complex disease, it is also important to associate this increased drug availability with the modification of schizophrenia symptoms in rodent models that replicate brain pathologies and behavioral abnormalities associated with schizophrenia in humans.[135] Among the cited literature, only 4 studies[70,82,85,99] associated the bioavailability of the drug with modification of the schizophrenia symptoms, while the majority of the studies limited its analysis to evaluate the nano-DDS formulation *in vivo* pharmacokinetics. Three of those studies[82,85,99] tested the nano-DDS formulations on apomorphine-induced schizophrenia behavior mice, while one[70] tested on amphetamine-induced psychosis behavior mice. All of them indicated significant decrease of the schizophrenia symptoms up to 48 h after the administration compared to the free drug (up to 8 h). However, since those were the minority of the studies, new studies should evaluate whether their formulations are able to change the pathological behavior symptoms associated with schizophrenia.

Transport across the blood–brain barrier

The blood–brain barrier (BBB) is a biological barrier of cells and the principal interface between the blood and the interstitial fluid that bathes the synaptic connection of the brain parenchyma. It is responsible for protecting the brain of toxins, parasites and other ill effects by a series of additional properties that allow it to tightly regulate the movement of molecules, ions, and cells between the blood and the central nervous system.[136–138] The BBB is basically formed by 3 major cells: the endothelial cells, the pericytes and the astrocytes. The endothelial cells are the cells that form the capillary tubule, and, on the BBB, they have the unique property of tightly regulating the movement of ions, molecules, and cells between the blood and the brain, when compared to the endothelial cells of other tissues, as they are tightly held together by tight junctions. Pericytes are cells that sit on the abluminal surface of the microvascular endothelial tube and have the ability to contract and control the diameter of the capillary. Interestingly, within the BBB, there is a higher ratio of endothelial cells:pericytes (between 1:1 to 3:1) than in the muscular tissue, which has a ratio of 100:1. This grants a higher ability to control the diameter and, thus the amount of blood passing through the brain. Finally, astrocytes are a major glial cell type which provides a link between the neuronal circuitry and the blood vessels and, also, tightly control the water homeostasis of the brain.[138] In this sense, the BBB is a formidable and efficient biological barrier designated to regulate the entry of several substances, including therapeutic molecules.[1,139]

Because of this special requirement, many newly discovered drugs for the central nervous system fail to enter the market, as they are unable to cross the BBB[136] as it is estimated that ~98% of all small molecules are not transported through the barrier.[137] Thus, the BBB is a major obstacle for the development of new

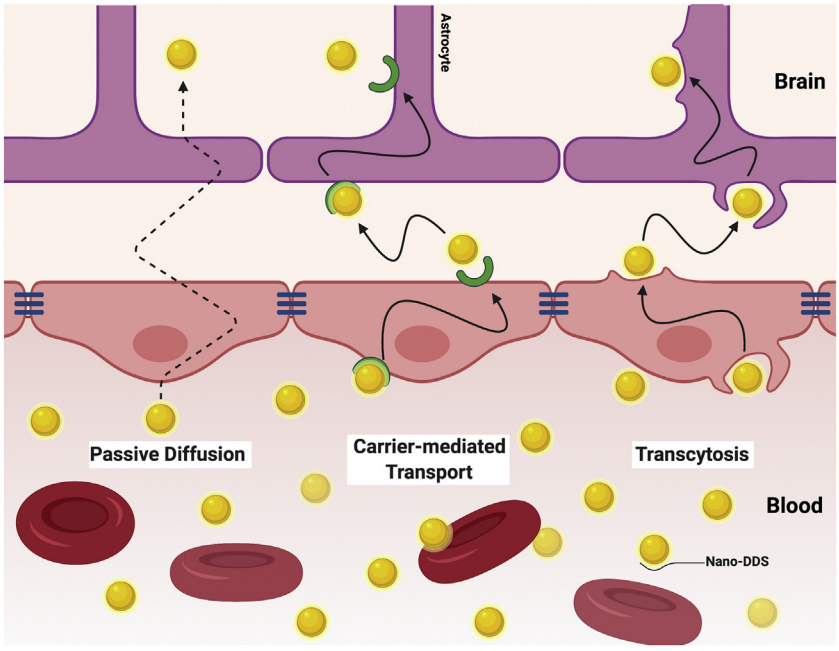

Figure 11. Three main routes by which drug delivery systems can use to cross the BBB: passive diffusion, carrier mediated transport and endocytosis/transcytosis pathways. Created with BioRender.

therapeutics targeting the brain.[79] Therefore, novel approaches to enable nanoparticles and drugs to actively pass the BBB and further into the brain are highly wanted.[140]

To do so, any new candidate drug is assessed for their BBB permeability.[141] Thus, a similar approach needs to be done to fully understand the nano-DDS potential to deliver the psychoactive drugs across the BBB. Two golden standards to estimate this are by the logarithm ratio of the drug concentration in the brain by the drug concentration in the blood (Log BB), and the permeability surface-area product (LogPS).[141–144] Log BB describes the overall extent of brain exposure to the drug at a steady state, while LogPS is indeed a perfusion method at the brain, and provides a direct measurement of the BBB apparent permeability.[141] Among the cited literature, only Esposito et al[133] evaluated the BBB permeation of their nano-DDS. Thus, more studies related to these permeation parameters of nano-DDS devices need to be done before proceeding into the stages of research. In this sense, computational modeling can assist this evaluation by predicting the drug permeability *in silico*.[141,145]

There are three main routes by which drug delivery systems can use to cross the BBB: passive diffusion, carrier mediated transport and endocytosis/transcytosis pathways,[1,136] as shown in Figure 11. Psychoactive drugs usually cross the BBB by passive diffusion due to favorable lipophilic characteristics and small molecular weight,[1,146] but they can be also transported by transcellular routes,[136] while water-soluble agents are usually transported by carrier mediated transport or endocytosis/transcytosis pathways, which are more complex than passive diffusion.[137] Therefore, for an antipsychotic drug to cross this biological barrier, it must have a certain level of lipophilicity.[1,137]

This lipophilicity requirement usually results in low aqueous solubility, which can cause issues to bioavailability and drug distribution. In this sense, nanopsychiatry can increase the bioavailability and aqueous solubility of high lipophilic drugs. Interestingly, Mendonça et al[147] and Durán-Lobato[124] demonstrate that SLN made of stearic acid, DOTAP and Pluronic F68 and polymeric nanoparticles made of PLGA are able to cross the BBB and are shown in the brain parenchyma. However, more studies are necessary for understanding the mechanism of how lipid and polymeric nanoparticles crosses the BBB, whether it is by active mechanisms or free diffusion and if they are able to deliver the drug in the brain (i.e. if they still possess the drug load and/or are not degraded).

Another approach is to use specific BBB transporters, such as the BBB choline transporter (BBB-ChT).[148,149] BBB-ChT is a transporter for choline for the synthesis of the cholinergic neurotransmitter acetylcholine[148] and might be suitable for drug delivery as the low choline plasma concentration (at a quarter of the enzyme Michaelis-Menten constant (K_m)).[149–151] Interestingly, nanoparticles do not necessarily need to be decorated with choline to activate the transport, as it has been suggested that quaternary ammonium and a free hydroxyl group are the key requirements for BBB-ChT substrate.[150] Moreover, it seems that bis-quaternary ammonium compounds can be used to achieve even higher affinity for this transporter than choline[150]; thus, decorating nanoparticle with these compounds might be useful to cross the BBB.

Thomsen et al,[140] on the other hand, propose use of magnetic force to guide magnetic iron nanoparticles to cross the barrier. This strategy seems interesting, but usage of magnetic iron nanoparticles seems to promote severe nanotoxicity *in vitro* and *in vivo*.[152]

Nanoparticles formulations

Pharmaceutical development of nanoparticulated formulations still has some limitations. Here we list the major challenges that nanopsychiatry might encounter with the nano-sized drug delivery system (nano-DDS), such as industrial scalable formulations and techniques, adequate characterization, formulation stability and formulation toxicity.

Industrial scalable production techniques

The first challenge on the nanoparticle formulation is the use of scalable production techniques. Although some progress has been developed, there is still a lack a scalable of drug delivery systems production techniques.[78,153,154] Most of the nanoparticle production techniques are considered bottom-up (i.e. starts from a dissolved molecule to a precipitate) and not top-down processes (i.e. starts from macro-size powder to be reduced). Bottom-up processes are less popular in the pharmaceutical industry as it requires difficult tasks to be done (e.g. removal of trace levels of the solvent) and desired features of the drug delivery systems can be lost during the scale up process.[153]

Emerging methods that have scale-up capabilities with minimal problems, such as membrane extrusion, supercritical fluid, microfluidizer and spray drying techniques, are available and have a few of their products placed in the market. However, use of these techniques for targeted and functionalized formulations at a large scale is still on debate.[153]

Adequate characterization

The second challenge that nanoparticles formulation might encounter is adequate characterization.

Although nano-DDS formulations are, in their majority, produced in water solutions/buffers, it is expected that these nano-DDS formulations interact with proteins, salts, and enzymes found in blood, saliva or any other components of body fluids. Proteins, in particular, can form two distinct and dynamic structures on nanoparticle surfaces: the hard and soft coronas. The hard coronas are proteins strongly bound to the nanoparticle surface, while the soft corona is made of loosely-bound proteins, possibly by protein–protein interactions.[155,156] Then, nano-DDS surfaces are modified upon body fluid entry and can substantially change and, thus, can influence the toxicity, distribution, metabolism, clearance, cellular fate and the overall nano-DDS biological response.[156]

Despite the fact that characterizing nano-DDS in buffer still may be used to initially access the nanoparticles characteristics and evaluate their drug delivery behaviors, it is essential to characterize the nanoparticle–corona complex in order to have the full picture of how nano-DDS will effectively behave in body fluids. Among all the articles cited here, none have analyzed the nanoparticle–corona complex.

However, this subject is still very complex and challenging, as it requires several techniques to fully characterize them.[157,158] Initially, it is necessary to determine the thickness of the corona layer. This can be done by using dynamic light scattering (DLS), differential centrifugal sedimentation (DCS), size exclusion chromatography (SEC) or transmission electron microscopy (TEM).

The next step, then, would be characterizing the nanoparticles corona. This requires techniques, such as poly(acrylamide) gel electrophoresis (PAGE) or liquid chormatography integrated to mass spectrometer (LC-MS/MS) to unveil the corona components.

Finally, it is necessary to estimate the affinities of the bound proteins with the nanomaterial surface, which can be accessed by circular dichroism spectroscopy (CD), fluorescence quenching and computational simulations for determining the conformation of the bound proteins; size exclusion chromatography (SEC), surface plasmon resonance (SPR) or isothermal titration calorimetry (ITC).

Stability

The third challenge that nanoparticles formulation might encounter is long term stability.[78] Technically, nanostructures can only exist for a finite period of time, as they are in as nanoscale objects present higher thermodynamic energy compared to their bulk materials counterparts under standard conditions. Therefore, nanoparticles should be considered as metastables, or, in another words, an energetically short-lived state compared to their bulk materials.[159] Nanoparticle stability usually describes the preservation of nanostructure regarding its shape, size, composition and surface chemistry[159–162]; subsequently, at least one of these stability components will always be in jeopardy due to the thermodynamic energy. Since most of the nano-DDSs seem to be nanostructures in solution-phase, size and surface chemistry of these nano-DDSs would be the first at risk as they undergo several collisions in the liquid medium. However, other effects, such as degradation of the nano-DDS composed materials or acidic/alkaline environment, might affect even more the nanoparticles' stability.

But for how long can these structures be stable? As described earlier, Duran-Lobato[122] demonstrated that all NLC formulations were stable after 2 months at 4 °C while Radaic et al[163] demonstrated that SLN formulation was stable for at least 5 month in 4 °C. More recently, Radaic et al reported SLN stability of over 3 years in 4 °C.[76] Most interestingly, Duran-Lobato[122] demonstrated that all NLC formulations were also stable in simulated intestinal conditions for 24 h. However, under 24 h of simulated gastric conditions, only the lecithin-coated nanoparticles remained stable. PLGA nanoparticles, on the other hand, start degrading after 6 h at 4 °C.[125]

Toxicity

Despite the numerous benefits of the nanocarriers, the fourth nano-DDS challenge is toxicity concerns, as the full toxicity potential of the nano-DDS was not properly evaluated yet.[20] Nano-DDS toxicity can emerge from undesirable interactions or events happening either inside or outside of the cells that promote morphological/structural, and biochemical alterations and/or genotoxicity.[15] These concerns are especially worrisome for schizophrenia patients, as they require long term dosage regimens.

However, despite these concerns, several studies have been demonstrating the safety of various nano-DDS formulations *in vitro*,[83,86,90,106,163,164] *ex vivo*[80,86,90] and *in vivo*.[80,86,90,103] [80,86,90,103,147,165,166] In this context, Mendonça et al,[147] seem to be one of the most extensive nanotoxicological evaluations of a nano-DDS formulation in vivo. The authors report that, despite

the transient acute inflammation response due to SLN intravenous administration, no significant toxicity was found in male Wistar mice, thus rendering the SLN formulation as safe. However, only acute toxicity has been addressed by these studies and extended studies regarding nano-DDS safety along many years of usage should be done.

Patient resistance

Patient resistance is another challenge for schizophrenia nanopsychiatry. It has been estimated that 20%-30% of the schizophrenia patients have treatment-resistant schizophrenia (TRS).[9,10] Often, mono-drug therapy for those TRS patients requires higher dosage of the drug, which can cause intolerable side effects and the need of continuous patient monitoring.[78] In this sense, nanopsychiatry can increase the bioavailability of the used drug without increasing the overall dosage, decreasing the potential side-effects of higher dosage.

Another alternative to this problem is the combination of two drugs for treatment. For instance, evidence suggests that lower dosage of clozapine in combination with risperidone is more effective and causes lesser side-effects than higher dosage of clozapine-alone treatment.[78] However, multidrug resistance (MDR) could become an issue using this approach for schizophrenia treatment. In this context, P-glycoprotein and BCRP might be involved in MDR. Shityakov et al[167] screened for in silico P-glycoprotein inhibitors using empirical scoring and found interesting results. However, as discussed before, *in vitro* and *in vivo* tests using adequate schizophrenia models need to be done to effectively check if the nano-DDS candidates are suitable or not against schizophrenia MDR. In this sense, nanopsychiatry is able to co-deliver drugs in lower concentration to treat TRS patients and avoid MDR.

Perspectives

Nanopsychiatry for schizophrenia diagnostics seems to be in its early stages; thus, many possibilities are still open to develop the field. Despite the advances already found in these works, improving the reliability of the sensors and decreasing even more the sensibilities and the minimal detection levels can open new ways and even revolutionize how to diagnose schizophrenia in the future, once these devices reach the market.

Nanopsychiatry for schizophrenia treatment seems to be more advanced than diagnostics counterpart, as one nano-DDS (Invega Sustenna®) was FDA approved in 2009. Nano-DDS enables the alteration of the pharmacokinetics and pharmacodynamics of the loaded-drug,[18] allowing, thus, to overcome several limitations of conventional schizophrenia treatment drugs. Throughout this work, several nano-DDSs demonstrated this potential, by increasing drugs' AUC,[12,70,72–75,86–88,92,94,95] [12,70,72–75,86–88,92,94,95,97,99–103] Cmax,[12,70,72,73,75,80,86,87,] [12,70,72,73,75,80,86,87,94,95,97,100,101,103] and Tmax,[12,80,87,88,] [12,80,87,88,92,95,97,100–103] increasing the BBB crossing,[84] or decreasing food interactions,[12,75] significantly decreased bodyweight gain[99] and catalepsy score[82,85,87] compared to free drug, and remarkably, inhibited apomorphine-induced psychosis behavior up to 72 h after the apomorphine injection, while the free drug inhibited only up to 8 h.[85,87]

Changing the pharmacokinetics and pharmacodynamics of drugs enables the increase of the efficiency of the treatment by increasing the drug accumulation in the target region. It has been estimated that there is a 100 to 500-fold increase of the drug accumulation in the target region using nano-DDS.[18,168] In this sense, nano-DDS enables the possibility of increasing the treatment efficacy via increasing the drug accumulation in the target region. Interestingly, it has already been demonstrated that there is a 2-fold increase in the brain targeting by using nano-DDS.[102]

Increasing the efficacy of schizophrenia treatments via nano-DDS enables the reduction of the injected dose and, thus, decreases the side effects,[18,168,169] including extra-pyramidal effects and teratogenic effects. Regarding the antipsychotic safety during pregnancy (teratogenic effects), until 2014, neither the first generation (typical) nor the second generation (atypical) antipsychotics have been adequately investigated towards teratogenicity.[170] This is very alarming as 4 antipsychotics (haloperidol, olanzapine, quetiapine and risperidone) have been described as able to cross the placenta, thus risking fetus psychotropic exposure.[171] Regarding this issue, nanopsychiatry is an important tool to resolve, as using nano-DDS seems to be safer from an asenapine teratogenic effect point of view, as it decreased the number of fetal birth defects by 2-fold when compared to the free drug.[103]

All these data point out a formidable assistance on schizophrenia treatment, by changing the pharmacokinetics/pharmacodynamics, increasing the efficiency of the treatment and, thus, increasing the safety of the treatments, especially regarding teratogenicity.

Also, we still expect for other promising drug delivery systems for schizophrenia treatment, such as cyclodextrin[172–174] and metal-organic frameworks (MOF).[175,176] Interestingly, to the best of our knowledge, MOF has only been tested as micrometer-sized drug delivery system (micro-DDS) and not as nano-DDS for schizophrenia treatment. For instance, de Freitas et al[177] demonstrated the incorporation of olanzapine on methyl-β-cyclodextrins by the loss of both olanzapine and methyl-β-cyclodextrin typical morphology, for instance. For instance, de Freitas et al. demonstrated that when olanzapine is incorporated in methyl-beta-cyclodextrins, both molecules loses their typical morphology, thus, increasing olanzapine water dissolution and stability.

Finally, we expect the merger of diagnostics and treatment devices, thus creating a theranostic device able to diagnose and treat schizophrenia patients at the same time,[69,178] depending on dopamine and/or serotonin levels. This might be possible by merging the dopamine and/or serotonin detectors with an antipsychotic nano-DDS.

Conclusion

As shown in this work, nanopsychiatry is able to develop devices capable of detecting patient levels of dopamine and serotonin, which per se, could improve the current schizophrenia

diagnostics as well as new nano-sized drug delivery systems (nano-DDS) which could improve schizophrenia treatment by increasing the efficacy and the pharmacokinetics of traditional schizophrenia drugs treatments. Besides that, nanopsychiatry is able to assist new ways to detect schizophrenia newfound biomarkers, either in the protein or gene levels and alternative treatments to reach the clinics.

Nanopsychiatry has great potential to revolutionize the actual schizophrenia diagnostics and treatment standards. Actually, it already produced one new schizophrenia treatment approved by the FDA for clinical use in 2009. Finally, it has been estimated that nanomedicine has the potential to save about 2 billion US dollars in the short-term, if these devices could access the market right now.[179]

References

1. Dening TJ, Rao S, Thomas N, Prestidge CA. Oral nanomedicine approaches for the treatment of psychiatric illnesses. *J Control Release* 2016;**223**:137-56.
2. Walker ER, McGee RE, Druss BG. Mortality in mental disorders and global disease burden implications. *JAMA Psychiatry* 2015;**72**:334-41.
3. Karim RS, et al. Mortality in hospital patients with and without mental disorders: a data-linkage cohort study. *J Psychiatr Res* 2019, https://doi.org/10.1016/j.jpsychires.2019.01.015.
4. Global Burden of Disease Cancer Collaboration *et al.* Global, regional, and national cancer incidence, mortality, years of life lost, years lived with disability, and disability-adjusted life-years for 32 cancer groups, 1990 to 2015: a systematic analysis for the Global Burden of Disease Study. *JAMA Oncol* **3,** 524–548 (2017).
5. Gururajan A, Malone DT. Does cannabidiol have a role in the treatment of schizophrenia? *Schizophr Res* 2016;**176**:281-90.
6. Chong HY, et al. Global economic burden of schizophrenia: a systematic review. *Neuropsychiatr Dis Treat* 2016;**12**:357-73.
7. McEvoy JP. The costs of schizophrenia. *J Clin Psychiatry* 2007;**68**:4-7.
8. Kumar S, Randhawa JK. Paliperidone-loaded spherical solid lipid nanoparticles. *RSC Adv* 2014;**4**:30186-92.
9. Dold M, Leucht S. Pharmacotherapy of treatment-resistant schizophrenia: a clinical perspective. *Evid Based Ment Health* 2014;**17**:33-7.
10. Lally J, Gaughran F, Timms P, Curran SR. Treatment-resistant schizophrenia: current insights on the pharmacogenomics of antipsychotics. *Pharmgenomics Pers Med* 2016;**9**:117-29.
11. Nascimento JM, Martins-De-Souza D. The proteome of schizophrenia. *NPJ Schizophr* 2015;**1**:14003.
12. Miao Y, Chen G, Ren L, Pingkai O. Characterization and evaluation of self-nanoemulsifying sustained-release pellet formulation of ziprasidone with enhanced bioavailability and no food effect. *Drug Deliv* 2016;**23**:2163-72.
13. Toumey C. The philosopher and the engineer. *Nat Nanotech* 2016;**11**:306-7.
14. Howard, K. A. in *Nanomedicine* **6,** 1–12 (Springer New York, 2016).
15. de Jesus, M. B. & Kapila, Y. L. in *Nanotoxicology* 201–227 (Springer, New York, NY, 2014). doi:10.1007/978-1-4614-8993-1_9.
16. Radaic A, de Jesus MB. Solid lipid nanoparticles release DNA upon endosomal acidification in human embryonic kidney cells. *Nanotechnology* 2018;**29**:1-10.
17. Murty BS, Shankar P, Raj B, Rath BB, Murday J. *Textbook of nanoscience and nanotechnology*. Berlin Heidelberg: Springer; 2013, https://doi.org/10.1007/978-3-642-28030-6.
18. Ventola CL. Progress in nanomedicine: approved and investigational nanodrugs. *P T* 2017;**42**:742-55.
19. Fond G, Macgregor A, Miot S. Nanopsychiatry—the potential role of nanotechnologies in the future of psychiatry: a systematic review. *Eur Neuropsychopharmacol* 2013;**23**:1067-71.
20. Dimitrijevic I, Pantic I. Application of nanoparticles in psychophysiology and psychiatry research. *Rev Adv Mater Sci* 2014;**38**:1-6.
21. Pantic I, Paunovic J, Dimitrijevic I, Pantic S. Gold nanomaterials in contemporary neurophysiology. *Neurology and Psychiatry Research Reviews on Advanced Materials Science* 2015;**40**:257-61.
22. Chandra P, Son NX, Noh H-B, Goyal RN, Shim Y-B. Investigation on the downregulation of dopamine by acetaminophen administration based on their simultaneous determination in urine. *Biosens Bioelectron* 2013;**39**:139-44.
23. Iswarya CN, Daniel SCGK, Sivakumar M. Studies on L-histidine capped Ag and Au nanoparticles for dopamine detection. *Mater Sci Eng C Mater Biol Appl* 2017;**75**:393-401.
24. Zaidi SA. Development of molecular imprinted polymers based strategies for the determination of Dopamine. *Sensors and Actuators B-Chemical* 2018;**265**:488-97.
25. Li C, Chen X, Zhang Z, Tang J, Zhang B. Gold nanoparticle-DNA conjugates enhanced determination of dopamine by aptamer-based microcantilever array sensor. *Sensors and Actuators B-Chemical* 2018;**275**:25-30.
26. Grunder, G. & Cumming, P. in *The neurobiology of schizophrenia* 109–124 (Elsevier, 2016). doi:10.1016/B978-0-12-801829-3.00015-X.
27. Seeman P, Kapur S. Schizophrenia: more dopamine, more D2 receptors. *Proc Natl Acad Sci U S A* 2000;**97**:7673-5.
28. Farjami E, et al. RNA Aptamer-based electrochemical biosensor for selective and label-free analysis of dopamine. *Anal Chem* 2013;**85**:121-8.
29. Zhang X, et al. Highly sensitive and selective detection of dopamine using one-pot synthesized highly photoluminescent silicon nanoparticles. *Anal Chem* 2015;**87**:3360-5.
30. Wang Z, Bai Y, Wei W, Xia N, Du Y. Magnetic Fe3O4-based sandwich-type biosensor using modified gold nanoparticles as colorimetric probes for the detection of dopamine. *Materials (Basel)* 2013;**6**:5690-9.
31. Biswal J, Misra N, Borde LC, Sabharwal S. Synthesis of silver nanoparticles in methacrylic acid solution by gamma radiolysis and their application for estimation of dopamine at low concentrations. *Radiat Phys Chem* 2013;**83**:67-73.
32. Qian T, Yu C, Wu S, Shen J. Gold nanoparticles coated polystyrene/reduced graphite oxide microspheres with improved dispersibility and electrical conductivity for dopamine detection. *Colloid Surf B* 2013;**112**:310-4.
33. Amiri M, Eynaki H, Mansoori Y. Cysteine-anchored receptor on carbon nanoparticles for dopamine sensing. *Electrochim Acta* 2014;**123**:362-8.
34. Qian T, Yu C, Zhou X, Wu S, Shen J. Au nanoparticles decorated polypyrrole/reduced graphene oxide hybrid sheets for ultrasensitiye dopamine detection. *Sensors and Actuators B-Chemical* 2014;**193**:759-63.
35. Leng Y, et al. Gold-nanoparticle-based colorimetric array for detection of dopamine in urine and serum. *Talanta* 2015;**139**:89-95.
36. Liu Y, Zhu W, Wu D, Wei Q. Electrochemical determination of dopamine in the presence of uric acid using palladium-loaded mesoporous Fe3O4 nanoparticles. *Measurement* 2015;**60**:1-5.
37. Zhang Y, et al. Rapid determination of dopamine in human plasma using a gold nanoparticle-based dual-mode sensing system. *Mater Sci Eng C Mater Biol Appl* 2016;**61**:207-13.
38. Khudaish EA, et al. Sensitive and selective dopamine sensor based on novel conjugated polymer decorated with gold nanoparticles. *J Electroanal Chem* 2016;**761**:80-8.
39. Liu Y, et al. Development of gold nanoparticle-sheathed glass capillary nanoelectrodes for sensitive detection of cerebral dopamine. *Biosens Bioelectron* 2015;**63**:262-8.

40. Alexander C, Bandyopadhyay K. Two dimensional palladium nanoparticle assemblies as electrochemical dopamine sensors. *Inorg Chim Acta* 2017;**468**:171-6.
41. Mei X, et al. Long-term stability of Au nanoparticle-anchored porous boron-doped diamond hybrid electrode for enhanced dopamine detection. *Electrochim Acta* 2018;**271**:84-91.
42. Rostami S, et al. Colorimetric sensing of dopamine using hexagonal silver nanoparticles decorated by task-specific pyridinum based ionic liquid. *Sensors and Actuators B-Chemical* 2018;**271**:64-72.
43. Lin J, Huang B, Dai Y, Wei J, Chen Y. Chiral ZnO nanoparticles for detection of dopamine. *Mater Sci Eng C Mater Biol Appl* 2018;**93**:739-45.
44. Qu F, Huang W, You J. A fluorescent sensor for detecting dopamine and tyrosinase activity by dual-emission carbon dots and gold nanoparticles. *Colloid Surf B* 2018;**162**:212-9.
45. Shobin LR, Sastikumar D, Manivannan S. Glycerol mediated synthesis of silver nanowires for room temperature ammonia vapor sensing. *Sensors Actuators A Phys* 2014;**214**:74-80.
46. Liao C, Zhang M, Niu L, Zheng Z, Yan F. Organic electrochemical transistors with graphene-modified gate electrodes for highly sensitive and selective dopamine sensors. *J Mater Chem B* 2014;**2**:191-200.
47. Quednow, B. B., Geyer, M. A. & Halberstadt, A. L. in *Handbook of behavioral neuroscience* **21,** 585–620 (Elsevier, 2010).
48. Shah, U. H. & González-Maeso, J. Serotonin and glutamate interactions in preclinical schizophrenia models. *ACS Chem Neurosci* acschemneuro.9b00044 (2019). doi:10.1021/acschemneuro.9b00044.
49. Xue C, et al. Electrochemical serotonin sensing interface based on double-layered membrane of reduced graphene oxide/polyaniline nanocomposites and molecularly imprinted polymers embedded with gold nanoparticles. *Sensors and Actuators B-Chemical* 2014;**196**:57-63.
50. Cesarino I, Galesco HV, Machado SAS. Determination of serotonin on platinum electrode modified with carbon nanotubes/polypyrrole/silver nanoparticles nanohybrid. *Mater Sci Eng C Mater Biol Appl* 2014;**40**:49-54.
51. Chavez JL, Hagen JA, Kelley-Loughnane N. Fast and selective plasmonic serotonin detection with aptamer-gold nanoparticle conjugates. *Sensors (Basel)* 2017;**17**.
52. Ran G, Chen X, Xia Y. Electrochemical detection of serotonin based on a poly(bromocresol green) film and Fe3O4 nanoparticles in a chitosan matrix. *RSC Adv* 2017;**7**:1847-51.
53. Terti M, et al. Highly selective electrochemical detection of serotonin on polypyrrole and gold nanoparticles-based 3D architecture. *Electrochem Commun* 2017;**75**:43-7.
54. Anithaa AC, Asokan K, Sekar C. Highly sensitive and selective serotonin sensor based on gamma ray irradiated tungsten trioxide nanoparticles. *Sensors and Actuators B-Chemical* 2017;**238**:667-75.
55. Swain BC, Mishra PP, Mishra H, Tripathy U. Monitoring the binding of serotonin to silver nanoparticles: a fluorescence spectroscopic investigation. *J Photochem Photobiol A Chem* 2018;**367**:219-25.
56. Godoy-Reyes TM, et al. Selective and sensitive colorimetric detection of the neurotransmitter serotonin based on the aggregation of bifunctionalised gold nanoparticles. *Sensors and Actuators B-Chemical* 2018;**258**:829-35.
57. Pries, L.-K., Guloksuz, S. & Kenis, G. in *Advances in experimental medicine and biology: proteomics, metabolomics, interactomics and systems biology* (ed. Delgado-Morales, R.) **978,** 211–236 (Neuroepigenomics in aging and disease, 2017).
58. Zong X, et al. DNA methylation in schizophrenia: progress and challenges. *Sci Bull* 2015;**60**:149-55.
59. Shimabukuro M, et al. Global hypomethylation of peripheral leukocyte DNA in male patients with schizophrenia: a potential link between epigenetics and schizophrenia. *J Psychiatr Res* 2007;**41**:1042-6.
60. Bailey VJ, et al. MS-qFRET: a quantum dot-based method for analysis of DNA methylation. *Genome Res* 2009;**19**:1455-61.
61. Bailey VJ, et al. DNA methylation detection using MS-qFRET, a quantum dot-based nanoassay. *Methods* 2010;**52**:237-41.
62. Wang Y, Zhang Y, Guo Y, Kang X-F. Fast and precise detection of DNA methylation with tetramethylammonium-filled nanopore. *Sci Rep* 2017;**7**:183.
63. Pollak TA, et al. Antibodies in the diagnosis, prognosis, and prediction of psychotic disorders. *Schizophr Bull* 2018;**64**:1123.
64. Ashton JR, Gottlin EB, Patz EFJ, West JL, Badea CT. A comparative analysis of EGFR-targeting antibodies for gold nanoparticle CT imaging of lung cancer. *PLoS ONE* 2018;**13**.
65. Dazzan P, et al. Different effects of typical and atypical antipsychotics on grey matter in first episode psychosis: the AESOP study. *Neuropsychopharmacology* 2005;**30**:765-74.
66. Meltzer H. What's atypical about atypical antipsychotic drugs? *Curr Opin Pharmacol* 2004;**4**:53-7.
67. Allen TM, Cullis PR. Drug delivery systems: entering the mainstream. *Science* 2004;**303**:1818-22.
68. Chue P, Chue J. A review of paliperidone palmitate. *Expert Rev Neurother* 2012;**12**:1383-97.
69. Muthu MS, Agrawal P, Singh RP. Antipsychotic nanomedicine: a successful platform for clinical use. *Nanomedicine (London)* 2014;**9**:2071-4.
70. Vieira SM, et al. A surface modification of clozapine-loaded nanocapsules improves their efficacy: a study of formulation development and biological assessment. *Colloid Surf B* 2016;**145**:748-56.
71. Shah B, Khunt D, Misra M, Padh H. Application of Box-Behnken design for optimization and development of quetiapine fumarate loaded chitosan nanoparticles for brain delivery via intranasal route*. *Int J Biol Macromol* 2016;**89**:206-18.
72. Narala A, Veerabrahma K. Preparation, characterization and evaluation of quetiapine fumarate solid lipid nanoparticles to improve the oral bioavailability. *J Pharm (Cairo)* 2013;**2013**:265741-7.
73. Shikha L, Sumit S, Murthy R. Formulation and evaluation of solid lipid nanoparticles of quetiapine fumarate and quetiapine hemifumarate for brain delivery in rat model. *Pharm Nanotechnol* 2013;**1**:239-47.
74. Aboti P, Shah P, Patel D, Dalwadi S. Quetiapine fumarate loaded solid lipid nanoparticles for improved oral bioavailability. *Drug Deliv Lett* 2014;**4**:170-84.
75. Miao Y, Sun J, Chen G, Lili R, Ouyang P. Enhanced oral bioavailability of lurasidone by self-nanoemulsifying drug delivery system in fasted state. *Drug Dev Ind Pharm* 2015;**42**:1234-40.
76. Radaic, A. *et al.* in *Advances in biomembranes and lipid self-assembly* **24,** 1–42 (Elsevier, 2016).
77. Halayqa M, Domańska U. PLGA biodegradable nanoparticles containing perphenazine or chlorpromazine hydrochloride: effect of formulation and release. *Int J Mol Sci* 2014;**15**:23909-23.
78. Panda A, Meena J, Katara R, Majumdar DK. Formulation and characterization of clozapine and risperidone co-entrapped spray-dried PLGA nanoparticles. *Pharm Dev Technol* 2016;**21**:43-53.
79. Piazza, J. *et al.* Haloperidol-loaded intranasally administered lectin functionalized poly(ethylene glycol)-block-poly(D,L)-lactic-co-glycolic acid (PEG-PLGA) nanoparticles for the treatment of schizophrenia. Eur J Pharm Biopharm 87**,** 30–39 (2014).
80. Seju U, Kumar A, Sawant KK. Development and evaluation of olanzapine-loaded PLGA nanoparticles for nose-to-brain delivery: in vitro and in vivo studies. *Acta Biomater* 2011;**7**:4169-76.
81. Center for Drug Evaluation Research. *Invega Sustenna pharmacology review*. 1–123 (2009).
82. Muthu MS, Rawat MK, Mishra A, Singh S. PLGA nanoparticle formulations of risperidone: preparation and neuropharmacological evaluation. *Nanomedicine-UK* 2009;**5**:323-33.
83. Lukasiewicz S, et al. Encapsulation of clozapine in polymeric nanocapsules and its biological effects. *Colloid Surf B* 2016;**140**:342-52.
84. Lukasiewicz S, et al. The interaction of clozapine loaded nanocapsules with the hCMEC/D3 cells — in vitro model of blood brain barrier. *Colloid Surf B* 2017;**159**:200-10.

85. Muthu MS, Singh S. Studies on biodegradable polymeric nanoparticles of risperidone: in vitro and in vivo evaluation. *Nanomedicine (London)* 2008;**3**:305-19.
86. Sawant K, Pandey A, Patel S. Aripiprazole loaded poly(caprolactone) nanoparticles: Optimization and in vivo pharmacokinetics. *Mater Sci Eng C Mater Biol Appl* 2016;**66**:230-43.
87. Joseph E, Reddi S, Rinwa V, Balwani G, Saha R. DoE based olanzapine loaded poly-caprolactone nanoparticles decreases extrapyramidal effects in rodent model. *Int J Pharm* 2018;**541**:198-205.
88. Alzubaidi AFA, El-Helw A-RM, Ahmed TA, Ahmed OAA. The use of experimental design in the optimization of risperidone biodegradable nanoparticles: in vitro and in vivo study. *Artif Cells Nanomed Biotechnol* 2017;**45**:313-20.
89. Dong B, Hadinoto K. Amorphous nanoparticle complex of perphenazine and dextran sulfate as a new solubility enhancement strategy of antipsychotic perphenazine. *Drug Dev Ind Pharm* 2017;**43**:996-1002.
90. Ruby, J. & Pandey, V. Formulation and evaluation of olanzapine loaded chitosan nanoparticles for nose to brain targeting an in vitro and ex vivo toxicity study. *Journal of Applied Pharmaceutical Science* 034–040 (2016). doi:10.7324/JAPS.2016.60905.
91. Patil PH, Wankhede PR, Mahajan HS, Zawar LR. Aripiprazole-loaded polymeric micelles: fabrication, optimization and evaluation using response surface method. *Recent Patents on Drug Delivery and Formulation* 2018;**12**:53-64.
92. Narayan R, et al. Development of risperidone liposomes for brain targeting through intranasal route. *Life Sci* 2016;**163**:38-45.
93. Venkateswarlu V, Manjunath K. Preparation, characterization and in vitro release kinetics of clozapine solid lipid nanoparticles. *J Control Release* 2004;**95**:627-38.
94. Manjunath K, Venkateswarlu V. Pharmacokinetics, tissue distribution and bioavailability of clozapine solid lipid nanoparticles after intravenous and intraduodenal administration. *J Control Release* 2005;**107**:215-28.
95. Sood S, Jawahar N, Jain K, Gowthamarajan K, Meyyanathan SN. Olanzapine loaded cationic solid lipid nanoparticles for improved oral bioavailability. *Curr Nanosci* 2013;**9**:26-34.
96. Kumar S, Randhawa JK. Preparation and characterization of paliperidone loaded solid lipid nanoparticles. *Colloid Surf B* 2013;**102**:562-8.
97. Yasir M, Sara UVS. Solid lipid nanoparticles for nose to brain delivery of haloperidol: in vitro drug release and pharmacokinetics evaluation. *Acta Pharm Sin B* 2014;**4**:454-63.
98. Kumar S, Randhawa JK. Solid lipid nanoparticles of stearic acid for the drug delivery of paliperidone. *RSC Adv* 2015;**5**:68743-50.
99. Joseph E, Reddi S, Rinwa V, Balwani G, Saha R. Design and in vivo evaluation of solid lipid nanoparticulate systems of olanzapine for acute phase schizophrenia treatment: Investigations on antipsychotic potential and adverse effects. *Eur J Pharm Sci* 2017;**104**:315-25.
100. Natarajan J, Baskaran M, Humtsoe LC, Vadivelan R, Justin A. Enhanced brain targeting efficacy of olanzapine through solid lipid nanoparticles. *Artif Cells Nanomed Biotechnol* 2017;**45**:364-71.
101. Gambhire VM, Ranpise NS. Enhanced oral delivery of asenapine maleate from solid lipid nanoparticles: pharmacokinetic and brain distribution evaluations. *Asian J Pharm* 2018;**12**:152-61.
102. Mandpe L, Pokharkar V. Targeted brain delivery of iloperidone nanostructured lipid carriers following intranasal administration: *in vivo* pharmacokinetics and brain distribution studies. *J Nanopharm Drug Deliv* 2013;**1**:212-25.
103. Singh SK, et al. Glycol chitosan functionalized asenapine nanostructured lipid carriers for targeted brain delivery: pharmacokinetic and teratogenic assessment. *Int J Biol Macromol* 2018;**108**:1092-100.
104. Dondapati D, Srimathkandala MH, Sanka K, Bakshi V. Improved solubility and dissolution release profile of lurasidone by solid self-nanoemulsifying drug delivery system. *Anal Chem Lett* 2016;**6**:86-97.
105. Shah S, Parmar B, Soniwala M, Chavda J. Design, optimization, and evaluation of lurasidone hydrochloride nanocrystals. *AAPS PharmSciTech* 2016;**17**:1150-8.
106. Helal HM, Mortada SM, Sallam MA. Paliperidone-loaded nanolipomer system for sustained delivery and enhanced intestinal permeation: superiority to polymeric and solid lipid nanoparticles. *AAPS PharmSciTech* 2017;**18**:1946-59.
107. Huang X, Brazel CS. On the importance and mechanisms of burst release in matrix-controlled drug delivery systems. *J Control Release* 2001;**73**:121-36.
108. de Azevedo CR, et al. Modeling of the burst release from PLGA micro- and nanoparticles as function of physicochemical parameters and formulation characteristics. *Int J Pharm* 2017;**532**:229-40.
109. Ife AF, Harding IH, Shah RM, Palombo EA, Eldridge DS. Effect of pH and electrolytes on the colloidal stability of stearic acid-based lipid nanoparticles. *J Nanopart Res* 2018;**20**.
110. Ball, R. L., Bajaj, P. & Whitehead, K. A. Oral delivery of siRNA lipid nanoparticles: fate in the GI tract. *Sci Rep* **8,** –12 (2018).
111. Scheife, R. T. Protein binding: what does it mean? DICP 23**,** S27–S31 (1989).
112. Jain KK. An assessment of iloperidone for the treatment of schizophrenia. *Expert Opin Investig Drugs* 2000;**9**:2935-43.
113. Greenberg WM, Citrome L. Pharmacokinetics and pharmacodynamics of lurasidone hydrochloride, a second-generation antipsychotic: a systematic review of the published literature. *Clin Pharmacokinet* 2017;**56**:493-503.
114. Burston JJ, Woodhams SG. Endocannabinoid system and pain: an introduction. *Proc Nutr Soc* 2014;**73**:106-17.
115. Almeida V, et al. Role of the endocannabinoid and endovanilloid systems in an animal model of schizophrenia-related emotional processing/cognitive deficit. *Neuropharmacology* 2019;**155**:44-53.
116. Alger BE, Kim J. Supply and demand for endocannabinoids. *Trends Neurosci* 2011;**34**:304-15.
117. Klein TW, Newton CA. Therapeutic potential of cannabinoid-based drugs. *Adv Exp Med Biol* 2007;**601**:395-413.
118. Esposito E, Drechsler M, Cortesi R, Nastruzzi C. Encapsulation of cannabinoid drugs in nanostructured lipid carriers. *Eur J Pharm Biopharm* 2016;**102**:87-91.
119. Ruggiero RN, et al. Cannabinoids and vanilloids in schizophrenia: neurophysiological evidence and directions for basic research. *Front Pharmacol* 2017;**8**.
120. Gardin A, Kucher K, Kiese B, Appel-Dingemanse S. Cannabinoid receptor agonist 13, a novel cannabinoid agonist: first in human pharmacokinetics and safety. *Drug Metab Dispos* 2009;**37**:827-33.
121. Dziadulewicz EK, et al. Naphthalen-1-yl-(4-pentyloxynaphthalen-1-yl) methanone: a potent, orally bioavailable human CB1/CB2 dual agonist with antihyperalgesic properties and restricted central nervous system penetration. *J Med Chem* 2007;**50**:3851-6.
122. Durán-Lobato M, et al. Lipid nanoparticles as an emerging platform for cannabinoid delivery: physicochemical optimization and biocompatibility. *Drug Dev Ind Pharm* 2016;**42**:190-8.
123. Durán-Lobato M, Martín-Banderas L, Goncalves LMD, Fernández-Arévalo M, Almeida AJ. Comparative study of chitosan- and PEG-coated lipid and PLGA nanoparticles as oral delivery systems for cannabinoids. *J Nanopart Res* 2015;**17**.
124. Durán-Lobato M, et al. Enhanced cellular uptake and biodistribution of a synthetic cannabinoid loaded in surface-modified poly(lactic-co-glycolic acid) nanoparticles. *J Biomed Nanotechnol* 2014;**10**:1068-79.
125. Martín-Banderas L, et al. Cannabinoid derivate-loaded PLGA nanocarriers for oral administration: formulation, characterization, and cytotoxicity studies. *Int J Nanomedicine* 2012;**7**:5793-806.
126. de Jesus MB, et al. Inclusion of the helper lipid dioleoylphosphatidylethanolamine in solid lipid nanoparticles inhibits their transfection efficiency. *J Biomed Nanotechnol* 2014;**10**:355-65.
127. Freitas C, Müller RH. Correlation between long-term stability of solid lipid nanoparticles (SLN (TM)) and crystallinity of the lipid phase. *Eur J Pharm Biopharm* 1999;**47**:125-32.
128. Seely KA, et al. AM-251 and rimonabant act as direct antagonists at mu-opioid receptors: Implications for opioid/cannabinoid interaction studies. *Neuropharmacology* 2012;**63**:905-15.

129. Silvestri C, Di Marzo V. Second generation CB1 receptor blockers and other inhibitors of peripheral endocannabinoid overactivity and the rationale of their use against metabolic disorders. *Expert Opin Investig Drugs* 2012;**21**:1309-22.
130. Piomelli D, et al. Pharmacological profile of the selective FAAH inhibitor KDS-4103 (URB597). *CNS Drug Rev* 2006;**12**:21-38.
131. Levin R, et al. Antipsychotic profile of cannabidiol and rimonabant in an animal model of emotional context processing in schizophrenia. *Curr Pharm Des* 2012;**18**:4960-5.
132. Boggs DL, et al. Rimonabant for neurocognition in schizophrenia: a 16-week double blind randomized placebo controlled trial. *Schizophr Res* 2012;**134**:207-10.
133. Esposito E, et al. Cannabinoid antagonist in nanostructured lipid carriers (NLCs): design, characterization and in vivo study. *Mater Sci Eng C Mater Biol Appl* 2015;**48**:328-36.
134. Kulkarni AD, Patel HM, Surana SJ, Belgamwar VS, Pardeshi CV. Brain–blood ratio: implications in brain drug delivery. *Expert Opin Drug Deliv* 2016;**13**:85-92.
135. Winship IR, et al. An overview of animal models related to schizophrenia. *Can J Psychiatr* 2019;**64**:5-17.
136. Patel MM, Patel BM. Crossing the blood–brain barrier: recent advances in drug delivery to the brain. *CNS Drugs* 2017;**31**:109-33.
137. Pardridge WM. Drug transport across the blood–brain barrier. *J Cereb Blood Flow Metab* 2012;**32**:1959-72.
138. Daneman R, Prat A. The blood–brain barrier. *Cold Spring Harb Perspect Biol* 2015;**7**.
139. Chen Y, Liu L. Modern methods for delivery of drugs across the blood–brain barrier. *Adv Drug Deliv Rev* 2012;**64**:640-65.
140. Thomsen LB, Thomsen MS, Moos T. Targeted drug delivery to the brain using magnetic nanoparticles. *Ther Deliv* 2015;**6**:1145-55.
141. Carpenter TS, et al. A method to predict blood–brain barrier permeability of drug-like compounds using molecular dynamics simulations. *Biophys J* 2014;**107**:630-41.
142. Shityakov S, Neuhaus W, Dandekar T, Förster C. Analysing molecular polar surface descriptors to predict blood–brain barrier permeation. *Int J Comput Biol Drug Des* 2013;**6**:146-56.
143. Lozovaya N, et al. Selective suppression of excessive GluN2C expression rescues early epilepsy in a tuberous sclerosis murine model. *Nat Commun* 2014;**5** 4563–15.
144. Shityakov S, et al. Ionization states, cellular toxicity and molecular modeling studies of midazolam complexed with trimethyl-β-cyclodextrin. *Molecules* 2014;**19**:16861-76.
145. Vilar S, Chakrabarti M, Costanzi S. Prediction of passive blood–brain partitioning: straightforward and effective classification models based on in silico derived physicochemical descriptors. *J Mol Graph Model* 2010;**28**:899-903.
146. Wong HL, Wu XY, Bendayan R. Nanotechnological advances for the delivery of CNS therapeutics. *Adv Drug Deliv Rev* 2012;**64**:686-700.
147. Mendonça MCP, et al. The in vivo toxicological profile of cationic solid lipid nanoparticles. *Drug Deliv Transl Res* 2020;**10**:34-42.
148. Geldenhuys WJ, Allen DD. The blood–brain barrier choline transporter. *Cent Nerv Syst Agents Med Chem* 2012;**12**:95-9.
149. Shityakov S, Förster C. In silico predictive model to determine vector-mediated transport properties for the blood–brain barrier choline transporter. *Adv Appl Bioinforma Chem* 2014;**7**:23-36.
150. Li J, et al. Choline-derivate-modified nanoparticles for brain-targeting gene delivery. *Adv Mater Weinheim* 2011;**23**:4516-20.
151. Allen DD, Smith QR. Characterization of the blood–brain barrier choline transporter using the in situ rat brain perfusion technique. *J Neurochem* 2001;**76**:1032-41.
152. Pisanic, T. R., II, Jin, S. & Shubayev, V. I. in *Nanotoxicity* 397–425 (John Wiley & Sons, Ltd, 2009). doi:10.1002/9780470747803.ch20.
153. Paliwal R, Babu RJ, Palakurthi S. Nanomedicine scale-up technologies: feasibilities and challenges. *AAPS PharmSciTech* 2014;**15**:1527-34.
154. Rantanen J, Khinast J. The future of pharmaceutical manufacturing sciences. *J Pharm Sci* 2015;**104**:3612-38.
155. Balog S, et al. Characterizing nanoparticles in complex biological media and physiological fluids with depolarized dynamic light scattering. *Nanoscale* 2015;**7**:5991-7.
156. Brun E, Sicard-Roselli C. Could nanoparticle corona characterization help for biological consequence prediction? *Cancer Nanotechnol* 2014;**5**:7-13.
157. Ahsan, S. M., Rao, C. M. & Ahmad, M. F. in *Cellular and molecular toxicology of nanoparticles* **1048,** 175–198 (Springer International Publishing, 2018).
158. Walkey CD, Chan WCW. Understanding and controlling the interaction of nanomaterials with proteins in a physiological environment. *Chem Soc Rev* 2012;**41**:2780-99.
159. Phan HT, Haes AJ. What does nanoparticle stability mean? *J Phys Chem C* 2019;**123**:16495-507.
160. Xi W, Phan HT, Haes AJ. How to accurately predict solution-phase gold nanostar stability. *Anal Bioanal Chem* 2018;**410**:6113-23.
161. Szabo P, Zelko R. Formulation and stability aspects of nanosized solid drug delivery systems. *Curr Pharm Des* 2015;**21**:3148-57.
162. Levard C, Hotze EM, Lowry GV, Brown GEJ. Environmental transformations of silver nanoparticles: impact on stability and toxicity. *Environ Sci Technol* 2012;**46**:6900-14.
163. Radaic A, De Paula E, de Jesus MB. Factorial design and development of solid lipid nanoparticles (SLN) for gene delivery. *J Nanosci Nanotechnol* 2015;**15**:1793-800.
164. Ould-Ouali L, et al. Self-assembling PEG-p(CL-co-TMC) copolymers for oral delivery of poorly water-soluble drugs: a case study with risperidone. *J Control Release* 2005;**102**:657-68.
165. Blasi P, et al. Lipid nanoparticles for brain targeting III. *Long-term stability and in vivo toxicity Int J Pharm* 2013;**454**:316-23.
166. Abdelbary GA, Tadros MI. Brain targeting of olanzapine via intranasal delivery of core-shell difunctional block copolymer mixed nanomicellar carriers: in vitro characterization, ex vivo estimation of nasal toxicity and in vivo biodistribution studies. *Int J Pharm* 2013;**452**:300-10.
167. Shityakov S, Förster C. In silico structure-based screening of versatile P-glycoprotein inhibitors using polynomial empirical scoring functions. *Adv Appl Bioinforma Chem* 2014;**7**:1-9.
168. Wolfram J, et al. Safety of nanoparticles in medicine. *Curr Drug Targets* 2015;**16**:1671-81.
169. Sainz V, et al. Regulatory aspects on nanomedicines. *Biochem Biophys Res Commun* 2015;**468**:504-10.
170. Galbally M, Snellen M, Power J. Antipsychotic drugs in pregnancy: a review of their maternal and fetal effects. *Ther Adv Drug Saf* 2014;**5**:100-9.
171. Newport DJ, et al. Atypical antipsychotic administration during late pregnancy: Placental passage and obstetrical outcomes. *Am J Psychiatry* 2007;**164**:1214-20.
172. Agnihotri N, Chowdhury AD, De A. Non-enzymatic electrochemical detection of cholesterol using β-cyclodextrin functionalized graphene. *Biosens Bioelectron* 2015;**63**:212-7.
173. Tiwari G, Tiwari R, Rai AK. Cyclodextrins in delivery systems: applications. *J Pharm Bioallied Sci* 2010;**2**:72-9.
174. Shityakov S. Broscheit, J. & Foerster, C. alpha-Cyclodextrin dimer complexes of dopamine and levodopa derivatives to assess drug delivery to the central nervous system: ADME and molecular docking studies. *Int J Nanomedicine* 2012;**7**:3211-9.
175. Fang X, Zong B, Mao S. Metal-organic framework-based sensors for environmental contaminant sensing. *Nanomicro Lett* 2018;**10**:64.
176. Cao J, Li X, Tian H. Metal-organic framework (MOF)-based drug delivery. *Curr Med Chem* 2019;**26**:1-21.
177. de Freitas MR, et al. Inclusion complex of methyl-beta-cyclodextrin and olanzapine as potential drug delivery system for schizophrenia. *Carbohydr Polym* 2012;**89**:1095-100.
178. Horowitz PM, Chiocca EA. Nanotechnology-based strategies for the diagnosis and treatment of intracranial neoplasms. *World Neurosurg* 2013;**80**:53-5.
179. Flühmann B, Ntai I, Brorchard G, Simoens S, Mühlebach S. Nanomedicines: the magic bullets reaching their target? *Eur J Pharm Sci* 2018;**128**:73-80.